Ames, B. W. (1966) *Methods Enzymol. 8*, 115.
Anderson, V. E. (1981) Ph.D. Dissertation, University of Wisconsin.
Anderson, V. E., Weiss, P. M., & Cleland, W. W. (1984) *Biochemistry 23*, 2779.
Bahnson, B. J., & Anderson, V. E. (1989) *Biochemistry 28*, 4173.
Blanchard, J. S., & Cleland, W. W. (1980) *Biochemistry 19*, 4506.
Cleland, W. W. (1977) *Adv. Enzymol. Relat. Areas Mol. Biol. 45*, 273.
Cleland, W. W. (1979) *Methods Enzymol. 63*, 103.
Dunaway-Mariano, D., & Cleland, W. W. (1980) *Biochemistry 19*, 1506.
Faller, L. D., Baroundy, B. M., Johnson, A. M., & Euall, R. X. (1977) *Biochemistry 16*, 3864.
Grimshaw, C. E., Cook, P. F., & Cleland, W. W. (1981) *Biochemistry 20*, 5655.
Nielsen, A. T. (1969) in *The Chemistry of the Nitro and Nitroso Groups* (Feuer, H., Ed.) pp 49–386, John Wiley & Sons, New York.
O'Sullivan, W. J. (1969) in *Data for Biochemical Research* (Dawson, R., et al., Eds.) pp 423–434, Oxford University Press, New York.
Stec, B., & Lebioda, L. (1990) *J. Mol. Biol. 211*, 235.
Stubbe, J. A., & Kenyon, G. L. (1972) *Biochemistry 11*, 338.
Tiepel, J. W., Hass, G. M., & Hill, R. L. (1968) *J. Biol. Chem. 243*, 5684.
Wang, T., & Himoe, A. (1974) *J. Biol. Chem. 249*, 3895.
Weiss, P. M., Boerner, R. J., & Cleland, W. W. (1987) *J. Am. Chem. Soc. 109*, 7201.
Wold, F., & Ballou, C. E. (1957) *J. Biol. Chem. 227*, 301.

Kinetics of Oxidative Phosphorylation in *Paracoccus denitrificans*. 1. Mechanism of ATP Synthesis at the Active Site(s) of F_oF_1-ATPase†

Juan A. Pérez* and Stuart J. Ferguson
Department of Biochemistry, University of Oxford, South Parks Road, Oxford OX1 3QU, U.K.
Received August 9, 1989; Revised Manuscript Received July 25, 1990

ABSTRACT: (1) The rate of ATP synthesis during NADH-driven aerobic respiration has been measured in plasma membrane vesicles from *Paracoccus denitrificans* as a function of the concentration of the substrates, ADP and inorganic phosphate (P_i). In both cases, the response of the reaction to changes in the degree of saturation of the F_oF_1-ATPase generated a perfect Michaelian dependence which allowed the determination of the corresponding Michaelis constants, K_m^{ADP} and $K_m^{P_i}$. (2) These kinetic parameters possess a real mechanistic significance, as concluded from the partial reduction of the rate of phosphorylation by the energy-transfer inhibitor venturicidin and the consequent analysis of the results within the framework of the theory of metabolic control. (3) The same membrane vesicles, which catalyze very high rates of ATP synthesis, have been shown to support much lower rates of the exchange ATP $\rightleftharpoons$ P_i and negligible rates of ATP hydrolysis. Under similar conditions, the preparations are also capable of generating phosphorylation potentials, ΔG_P, of 60–61 kJ·mol^{-1}. (4) These properties have allowed analysis of the synthetic reaction in the presence of significant concentrations of the product, ATP, using integrated forms of the Michaelis–Menten rate equations. (5) It has been shown that ATP produces pure competitive product inhibition of the forward reaction with a value of $K_i^{ATP} = 16 \pm 1$ μM, thus indicating that the affinity of the nucleotide for the active site(s) of the F_oF_1-ATPase, during net ATP synthesis, is significantly higher than previously thought. (6) The order of binding of the substrates, ADP and P_i, to the active site(s) has been determined as random. (7) At very low concentrations of ADP, a second and much smaller Michaelis constant for this substrate has been identified, with an estimated value of $K_m^{ADP} \simeq 50$ nM, associated with a maximal rate of only 2% of that measured at a higher range of concentrations. (8) The results obtained are discussed in relation to the presence of two or three equivalent catalytic sites operating in the cooperative manner explicitly described by the binding change mechanism.

The ubiquitous enzyme F_oF_1-ATPase[1] completes the process of oxidative phosphorylation or photophosphorylation in mitochondria, chloroplasts, and many bacteria by catalyzing the synthesis of ATP from ADP and inorganic phosphate (P_i) driven by the energy stored in the protonmotive force, Δp [for review, see Senior (1988)]. Given the central role of this enzyme in energy transduction, an understanding of the mechanism of ATP synthesis and of the events that take place at the active site(s) of this enzyme seems essential. There are two important questions concerning ATP synthesis which demand a precise answer: (1) What is the order of binding for the substrates, ADP and P_i, at the active site(s) of the F_oF_1-ATPase? (ii) What is the affinity of the active site for the product, ATP, during net phosphorylation?

With regard to the second question, the binding change mechanism proposed for this enzyme [e.g., Kayalar et al. (1977), Gresser et al. (1982), and Boyer (1989)] indicates that

† J.A.P. was supported by a research fellowship from the Departamento de Educación, Universidades e Investigación, Gobierno Vasco/Eusko Jaurlaritza, Spain.

[1] Abbreviations: Δp, protonmotive force or transmembrane electrochemical proton gradient expressed in millivolts; $\Delta\psi$, transmembrane electrical potential; ΔpH, transmembrane pH gradient; P_i, inorganic phosphate; G6P, glucose 6-phosphate; HK, hexokinase; PK, pyruvate kinase; PEP, phosphoenolpyruvate; F_oF_1-ATPase, H^+-translocating ATPase type F_oF_1 (ATP-synthase; EC 3.6.1.3); F_1, soluble catalytic sector of F_oF_1-ATPase; FCCP, carbonyl cyanide *p*-(trifluoromethoxy)-phenylhydrazone.

0006-2960/90/0429-10503$02.50/0

energization has a very strong effect on the affinity for ATP, as observed experimentally; while in nonphosphorylating conditions the enzyme binds ATP at the active site very tightly (Grubmeyer et al., 1982; Penefsky, 1985a), the onset of ATP synthesis is accompanied by a strong promotion of the rate of release of the nucleotide, which dramatically reduces its affinity for the active site (Boyer et al., 1973; Penefsky, 1985b,c). The apparently very low affinity of the F_oF_1-ATPase from chloroplasts for ATP detected during photophosphorylation corroborates this view (Franek & Strotmann, 1981); it was found that ATP produces pure competitive product inhibition, corresponding to its binding at the active site, but given by an apparent inhibition constant only in the millimolar range (Franek & Strotmann, 1981). In principle, this behavior will account for the capacity of the F_oF_1-ATPase to drive net ATP synthesis efficiently even in the presence of large concentrations of the nucleotide, as occurs in most biological systems (Senior, 1988).

However, when a two-substrate enzyme such as the F_oF_1-ATPase is being dealt with (if we only take ADP and P_i into account), the real affinity for the product, as determined from product inhibition studies, can only be determined when the order of binding of the substrates is conclusively established (Rudolph, 1979; Cornish-Bowden, 1981). Previous reports on the order of binding of ADP and P_i have been contradictory; while either a random binding (Kayalar et al., 1977) or a compulsory order with P_i binding first (Schuster et al., 1977) has been proposed for the mitochondrial enzyme, the third possibility of a compulsory order with ADP binding first has been deduced for the F_oF_1-ATPase from chloroplasts (Selman & Selman-Reimer, 1981). Different methodologies were used in all three cases. Therefore, a clear answer obtained from more direct evidence is still needed.

One of the most direct ways of determining the order of binding for a two-substrate enzyme is with studies of product inhibition (Cornish-Bowden, 1981). We report in this paper such studies carried out with membrane preparations from the microorganism *Paracoccus denitrificans*. As shown here and previously reported (Ferguson et al., 1976; Harris et al., 1977), the F_oF_1-ATPase in vesicles from *P. denitrificans* is exceptionally well suited for product inhibition studies. This is due to the very low rates of ATP hydrolysis and ATP $\rightleftharpoons$ P_i exchange determined under all conditions, compared to very high rates of ATP synthesis.

Nevertheless, when analyzing the kinetics of ATP synthesis, it is important to consider first two factors that can substantially affect the mechanistic interpretation of the data: (i) in principle, real kinetic parameters such as V_{max} and K_m can only be obtained when single enzymes and not multienzymatic pathways are being dealt with (Stoner, 1984), which is the case with oxidative phosphorylation or photophosphorylation; (ii) there is involvement of more than one catalytic site in the F_oF_1-ATPase during the phosphorylating reaction, operating through the binding change mechanism proposed for the enzyme [e.g., Kayalar et al. (1977) and Gresser et al. (1982); for review, see also Cross (1981), Senior (1988), and Boyer (1989)]. Both factors can produce severe limitations for the application of simple Michaelis–Menten kinetics to ATP synthesis and need to be accounted for.

In line with the first point, Quick and Mills (1987, 1988) have highlighted the variations in Δp which take place during analyses of this sort. An alternative approach has been used in this paper which takes advantage of the analytical strength of the theory of metabolic control (Kacser & Burns, 1973; Heinrich & Rapoport, 1974). In short, it is shown that the value of the flux control coefficient of the F_oF_1-ATPase for the overall process of oxidative phosphorylation has a direct impact on the mechanistic significance of the experimental values of K_m^{ADP} and $K_m^{P_i}$.

Concerning the second point and in agreement with the binding change mechanism, recent reports have shown the presence of at least two different Michaelis constants for the substrates of the phosphorylating reaction in chloroplasts (Stroop & Boyer, 1985) and submitochondrial particles (Matsuno-Yagi & Hatefi, 1985, 1986; Hekman et al., 1988). In this paper, we also report the results of similar studies in *P. denitrificans* and discuss them in the light of the type and extent of product inhibition.

Materials and Methods

Experimental

Biological Materials. P. denitrificans (NCIB 8944) was grown anaerobically with succinate as the carbon source and nitrate as the electron acceptor (Burnell et al., 1975). Membrane vesicles were prepared as described (John, 1977) and stored under nitrogen as a suspension in 5 mM magnesium acetate and 10 mM Tris–acetate (pH 7.3) at a concentration of 10–15 mg of protein·mL^{-1}. Protein concentration was determined according to the method of Lowry et al. (1951). The respiratory and phosphorylating properties of the vesicles were routinely checked with a Clark-type oxygen electrode.

ATP Synthesis. To measure initial rates of phosphorylation, reactions were carried out in completely aerobic conditions at pH 7.3, with the temperature maintained at 30 °C. The ATP produced was determined as the ^{32}P incorporated into organic phosphate in the presence of glucose and yeast hexokinase. Esterified phosphate was separated from P_i according to the method of Sugino and Miyoshi (1964). In the assay conditions used, the precipitation of nonincorporated phosphate was essentially complete (≥99.98%).

When the Michaelis constant for ADP (K_m^{ADP}) was determined, the reaction mixture contained the following in a final volume of 2 mL: 10 mM [^{32}P]P_i/21 mM Tris (10–25 μCi·mL^{-1}; Amersham International) (pH 7.3), 5 mM magnesium acetate, 1% (v/v) ethanol, 0.1 mg of alcohol dehydrogenase·mL^{-1} (~20 units·mL^{-1}), 20 mM glucose, 0.45–0.55 mg of hexokinase·mL^{-1} (15–20 units·mL^{-1}), and 0.1–0.5 mg vesicle of protein·mL^{-1}. Respiration was initiated by the addition of 0.6 mM NAD^+, and 1 min later the phosphorylation reaction was started by the addition of varying amounts of MgADP. A total of eight aliquots of 50 μL were withdrawn at intervals of 30 s, and each aliquot was added to 0.5 mL of a chilled mixture containing 3% (w/v) ammonium molybdate, 0.6–0.7 M HCl, 2 mM EDTA, 1% (w/v) trichloroacetic acid, and 1% (v/v) triethylamine. After being mixed thoroughly, each sample was kept on ice for 5–10 min and centrifuged at room temperature (3 min, 10000*g*). Aliquots of 200 μL were taken from the supernatants and added to plastic vials containing 10 mL of 100 mM K_2HPO_4. The content of esterified [^{32}P]phosphate was determined by the Cerenkov method (counted for 2 min). Each set of samples was counted three times and the mean values taken, after correction for decay.

In order to determine the Michaelis constant for P_i ($K_m^{P_i}$), a slightly different protocol was followed. The reaction mixture (in a final volume of 4 mL) contained magnesium acetate, ethanol, alcohol dehydrogenase, glucose, hexokinase, and NAD^+ as before, together with 0.1–0.5 mg of vesicle protein·mL^{-1}, 21 mM Tris/HCl (pH 7.3), 0.5–0.7 mM [^{32}P]-NaH_2PO_4 (0.5–1.5 μCi·mL^{-1}), and a saturating amount of

MgADP. Respiration and phosphorylation were again initiated by the addition of NAD^+ and MgADP, respectively. A total of 18 aliquots of 100 μL were withdrawn at intervals of 20–50 s (chosen to follow the reaction until complete consumption of all the P_i) and treated as before, except that the plastic vials contained 10 mL of water only.

Product Inhibition. To study the effect of product inhibition on the phosphorylation reaction, when either ADP or P_i was present at a nonsaturating concentration, protocols as before were followed except that in both cases the total volume of the reaction mixture was 4 mL and this did not contain either hexokinase or glucose. When ADP was the limiting substrate, the initial concentration of added MgADP was 70–150 μM and the amount of membrane vesicles present only 10–50 μg of vesicle protein·mL^{-1}. A total of 18 aliquots of 100 μL were withdrawn from the reaction mixtures at intervals of 20–30 s and treated as before to determine the amount of ^{32}P incorporated into ATP. The inhibitory effect of ATP on the reaction was characterized by use of the initial concentrations of MgATP (0–10 mM) added simultaneously with the MgADP.

ATP ⇌ P_i Exchange. The same protocol was followed to determine the rate of ATP ⇌ P_i exchange, although MgADP was excluded and the incorporation of ^{32}P (10 mM P_i initially present) into organic phosphate was started by the addition of 10 mM MgATP. Due to the ADP contaminating the ATP, a limited and fast production of [γ-^{32}P]ATP was observed before thermodynamic equilibrium had been reached, followed by a linear and much lower rate of exchange.

ATP Hydrolysis. To measure the rate of ATP hydrolysis, reactions were carried out in completely aerobic conditions at 30 °C as before, and the rate of P_i production was measured by the method of Taussky and Shorr (1953). The reaction was started by addition of MgATP (final concentration 5 mM) to mixtures containing 21 mM Tris/HCl (pH 7.3), 5 mM magnesium acetate, and 0.05–0.06 or 0.5–0.6 mg of vesicle protein·mL^{-1}, together with other chemicals and enzymes depending on experimental conditions, to a volume of 3 or 4 mL, respectively. A total of five or four aliquots of 400 or 800 μL were withdrawn every 1 or 2 min, added to 0.5 mL of chilled trichloroacetic acid (25% w/v) with thorough mixing, kept on ice for 10 min, and centrifuged at room temperature (5 min, 10000*g*). Aliquots of 1 mL were taken from the supernatants and titrated for P_i content.

Other Experimental Conditions. Partial uncoupling of the membrane preparations was produced by addition of the uncoupler FCCP. Partial inhibition of the electron-transport chain was attained with rotenone (which inhibits the complex NADH dehydrogenase), myxothiazol (which blocks the bc_1 complex), or cyanide (which affects the terminal oxidases). Partial inactivation of the F_oF_1-ATPase was obtained by addition of the energy-transfer inhibitor venturicidin. Potassium cyanide was prepared in 21 mM Tris/HCl (pH 7.3) the same day it was used. The other effectors were added as ethanolic solutions. In all cases, the vesicles were incubated with the effector for at least 3 min before respiration was started.

Titrations. The solutions of P_i used were titrated by the method of Taussky and Shorr (1953). The solutions of ADP and ATP used were titrated by enzymatic methods [see Sorgato et al. (1981)]. The solutions of ATP were titrated for both ATP and contaminating ADP before and after the experiments. When necessary, the small contamination of ATP in the solutions of ADP was also titrated in a similar way.

Analysis of Kinetic Data

Initial Rates. When initial rates in the presence of hexokinase and glucose were obtained for a range of nonsaturating concentrations of ADP, the resulting data were analyzed by means of Hanes plots of [ADP]/v vs v, where v represents the initial rate, or by means of Eadie–Hofstee plots of v vs v/[ADP]. However, it was difficult to measure initial rates of phosphorylation when a nonsaturating concentration of P_i was used, as this substrate was not regenerated by the presence of hexokinase and glucose (see Results). For this reason, the resulting nonlinear progress curves were used to analyze the reaction by means of the integrated form of the appropriate Michaelis–Menten equation (Cornish-Bowden, 1981). Given a high and saturating concentration of ADP (kept constant throughout), the following equation applied:[2]

$$t/\ln (a/a_o) = K_m^{P_i}/V_{max} + (1/V_{max})[(a_o - a)/\ln (a_o/a)] \quad (1)$$

where t is the time of reaction and $a \equiv [P_i]$. As hexokinase does not permit the presence of significant concentrations of ATP, so eliminating any possibility of product inhibition, the graphical representation of $t/\ln (a_o/a)$ vs $(a_o - a)/\ln (a_o/a)$ was equivalent to a Hanes plot of a/v vs a, v being the initial rate associated with each concentration a. Therefore, the data from the progress curve could be plotted according to eq 1, to produce a set of parameters (V_{max}, $K_m^{P_i}$) identical with those which could be extracted from a normal Hanes plot (Cornish-Bowden, 1981). The correct use of eq 1 to linearize data from progress curves has been previously discussed by others (Atkins & Nimmo, 1973; Orsi & Tipton, 1979).

Product Inhibition. The progress curves corresponding to the reactions of ATP synthesis which were carried out in the absence of hexokinase and glucose could not be analyzed with classical initial rate kinetics. Again, integrated forms of the appropriate Michaelis–Menten rate equations had to be used (Cornish-Bowden, 1981). When no initial ATP was present, the progress curves could be linearized as before by means of

$$t/\ln (s_o/s) = {}^{app}K_m/{}^{app}V_{max} + (1/{}^{app}V_{max})[(s_o - s)/\ln (s_o/s)] \quad (2)$$

where s represents the concentration of the nonsaturating substrate at a given time and s_o is the initial concentration of that substrate. The symbols ${}^{app}K_m$ and ${}^{app}V_{max}$ represent the associated kinetic parameters, which could be determined by constructing the corresponding representation of $t/\ln (s_o/s)$ vs $(s_o - s)/\ln (s_o/s)$. These parameters are only apparent, as their values depend directly on the "real" ones,[3] K_m and V_{max}, and on the type and extent of product inhibition (Cornish-Bowden, 1981; see Results).

In the presence of initially large concentrations of ATP, eq 2 could not be successfully used, due to the marked increases

[2] In this and the following paper, when convenient, the reaction of ATP synthesis is often written as A + B ⇌ P, where A ≡ P_i, B ≡ ADP, and P ≡ ATP. Thus, K_m^A symbolizes the Michaelis constant for P_i etc., a symbolizes [P_i], and b represents [ADP]; a_o and b_o represent the initial concentrations of substrates in the reaction mixtures; p symbolizes the concentration of newly synthesized ATP; p_o represents the ATP initially added to the reaction mixtures.

[3] For simplicity of presentation, in this and the following paper the term "apparent" applied to K_m or V_{max} (i.e., ${}^{app}K_m$ or ${}^{app}V_{max}$) is mainly used when referring to the values extracted from reactions where product inhibition occurs. Therefore, the symbols K_m and V_{max} ("real" parameters) are used to represent the values extracted from reactions where initial rates are measured and product inhibition is absent. In principle, the real parameters K_m and V_{max} can only be considered when dealing with single enzymes (see above). However, as shown in this paper (Appendix I), such a simplification remains valid for the Michaelis constants for ADP and P_i during ATP synthesis catalyzed by the F_oF_1-ATPase of *P. denitrificans* under the experimental conditions described here.

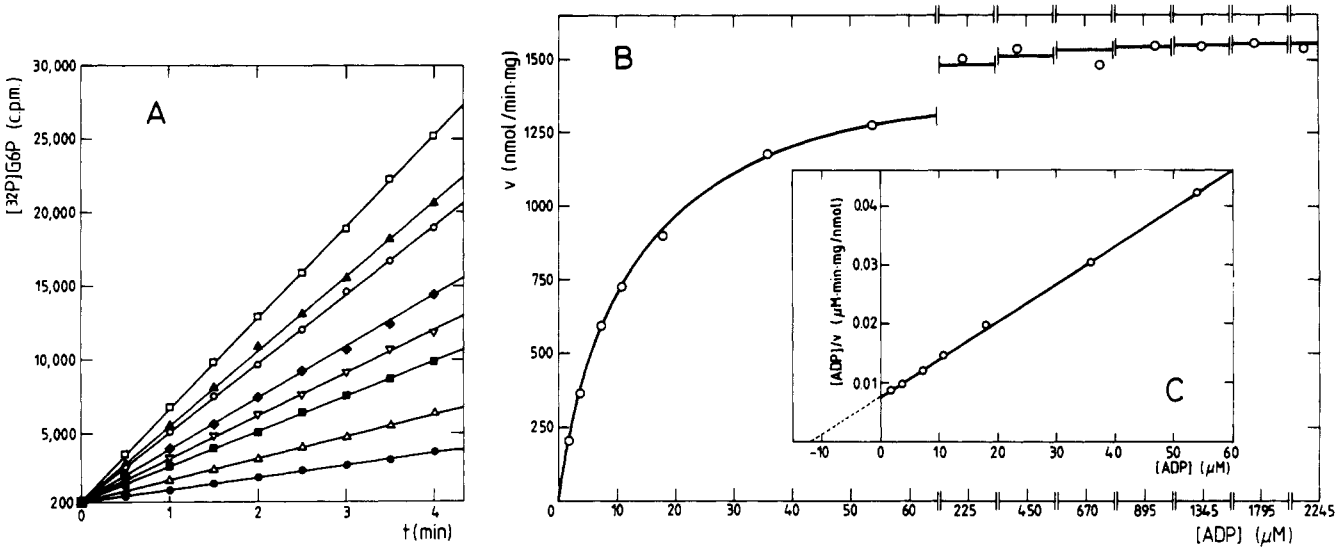

FIGURE 1: ATP synthesis in *P. denitrificans*. Determination of K_m^{ADP}. The rate of phosphorylation by inside-out vesicles of the plasma membrane of *P. denitrificans* (0.19 mg of protein·mL^{-1}) was measured in the presence of 10 mM [^{32}P]P_i and various concentrations of ADP (1.8–2243 μM), as described under Materials and Methods. (A) Time-dependent incorporation of ^{32}P into glucose 6-phosphate (G6P). The rates of ATP synthesis for each concentration of ADP were obtained by linear regression of the production of [^{32}P]G6P. The data shown correspond to the concentrations of ADP: 1.8 (●), 3.6 (△), 7.2 (■), 10.8 (▽), 17.9 (◆), 35.9 (○), 53.8 (▲), and 897 μM (□). (B) The rates of phosphorylation, v, are plotted against [ADP]. (C) A Hanes plot of [ADP]/v vs [ADP] is used to extract the value of the kinetic parameters V_{max} and K_m^{ADP} [V_{max} = 1560 nmol of ATP·min^{-1}·(mg of protein)$^{-1}$ and K_m^{ADP} = 12.0 μM]. The solid line included in the primary plot of v vs [ADP] (panel B) represents the rectangular hyperbola derived from these parameters.

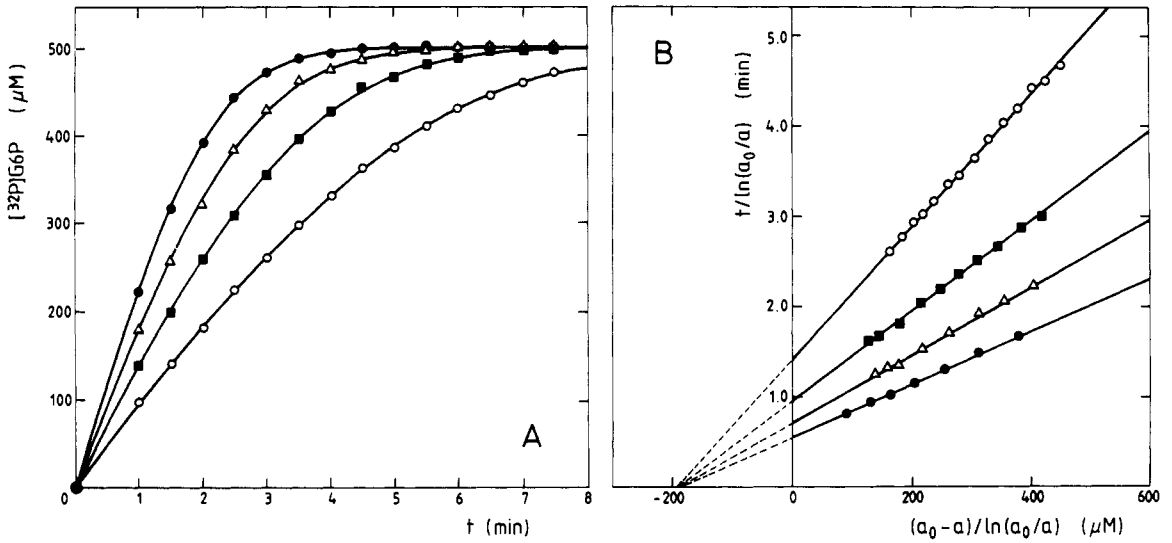

FIGURE 2: ATP synthesis in *P. denitrificans*. Determination of K_m^{Pi}. (A) The rate of phosphorylation by inside-out vesicles of the plasma membrane of *P. denitrificans* (0.15 mg of protein·mL^{-1}) was measured in the presence of a nonsaturating concentration of [^{32}P]P_i (0.5 mM) and a range of nonsaturating concentrations of ADP, as described under Materials and Methods. The figure shows the time-dependent incorporation of ^{32}P into G6P. The concentrations of ADP added were 3.7 (○), 7.4 (■), 18.6 (△), and 37.2 μM (●). (B) The data from the progress curves were represented according to eq 1 (see Materials and Methods) where $a \equiv [P_i]$: The family of lines have a common intercept in the x axis, indicating that $K_m^{Pi} = K_i^{Pi}$ (=190 μM).

in the value of $^{app}K_m$ (see Results). A different approach had to be applied according to the original method by Fernley (1974). Equation 2 can be rearranged as

$$^{app}V_{max}t - p = {}^{app}K_m(\ln [s_o/(s_o - p)]) \quad (3)$$

where p ($=s_o - s$) represents the concentration of newly synthesized product at a given time. Given the set of values (t, p) of the progress curve, eq 3 can be used to take successive estimates of $^{app}K_m$ and/or $^{app}V_{max}$ and to obtain the corresponding sums of squares of the resulting standard deviations. An iterating procedure has to be followed until the pair ($^{app}K_m$, $^{app}V_{max}$) which produces the minimal sum of squares of the standard deviations is obtained (Fernley, 1974). In our case, when high concentrations of ATP were present and large values of $^{app}K_m$ generated, the method by Fernley was also unable to produce simultaneous and precise estimates of both $^{app}K_m$ and $^{app}V_{max}$, so pure competitive product inhibition was assumed and a fixed value for $^{app}V_{max}$ taken (see Results). All the calculations involving eq 3 were carried out on a 3/110 computer (Sun Microsystems) operated in C language.

Results

Michaelian Kinetics of ATP Synthesis. The hyperbolic response of the rate of ATP synthesis by F_oF_1-ATPases to changes in the concentration of the substrates ADP and P_i is widely documented [e.g., Kayalar et al. (1976) and Selman and Selman-Reimer (1981)]. As shown here (Figures 1 and 2), oxidative phosphorylation catalyzed by inside-out vesicles of the plasma membrane of *P. denitrificans* gives rise to the same observation. With saturating concentrations of P_i and

nonsaturating concentrations of ADP (Figure 1), the presence of hexokinase and glucose allows the linear production of organic phosphate to be followed (Figure 1A). The rates obtained can be plotted against [ADP], generating a perfect hyperbolic response (Figure 1, panels B and C). It is important to notice that, for the range of [ADP] examined (2–2240 μM), only one V_{max} and one K_m^{ADP} can be observed.

When nonsaturating and low concentrations of P_i are used, the production of organic phosphate is no longer linear (Figure 2A). As described under Materials and Methods, the analysis of the progress curves can be carried out by means of the integrated Michaelis–Menten equation, thus generating linear plots of $t/\ln(a_o/a)$ vs $(a_o - a)/\ln(a_o/a)$ (Figure 2B). For the correct analysis of the experiments of product inhibition presented in this paper, it was essential to determine the relationship between the values of K_m^{ADP} and $K_m^{P_i}$ and the dissociation constants K_i^{ADP} and $K_i^{P_i}$ for binding of both substrates to the F_oF_1-ATPase (see Appendix II). This could be easily derived from the progress curves of Figure 2A, which were obtained in the presence of a range of nonsaturating concentrations of ADP. The plots according to eq 1 produce a family of lines with a common intercept on the x axis, therefore indicating that $K_m^{P_i} = K_i^{P_i}$ (Figure 2B). Secondary plots for the slopes and the intercepts with the y axis can also be constructed (not shown), confirming that $K_m^{ADP} = K_i^{ADP}$ (Appendix II).

Figures 1 and 2 are representative of data obtained with more than 15 different vesicle preparations. A certain variability of the determined parameters was observed depending on the preparation of vesicles used. However, the ranges of values obtained [K_m^{ADP} = 7–13 μM; $K_m^{P_i}$ = 0.15–0.35 mM; V_{max} = 0.7–2.8 μmol of ATP·min^{-1}·(mg of protein)$^{-1}$], particularly wide in the case of the maximal rate V_{max}, were not a consequence of any significant variation in the degree of coupling of the membrane. This possibility was discounted because the variations in the rate of phosphorylation were always matched by parallel differences in rates of respiration at various states, while the "ADP/O" ratio and respiratory control ratios (Nicholls, 1982) were all remarkably constant (not shown). A plausible explanation is offered by variations in yields between vesicle populations of opposite orientations, "inside out" versus "right side out" (Burnell et al., 1975; McCarthy & Ferguson, 1983).

Application of Control Theory to the F_oF_1-ATPase from P. denitrificans. The Michaelian dependence of the rate of phosphorylation on substrate concentration illustrated in Figures 1 and 2 prompts considerations about the mechanistic significance of the parameters V_{max}, K_m^{ADP}, and $K_m^{P_i}$ determined experimentally. A relevant answer can be provided by the effect on these parameters of partial inhibition of the F_oF_1-ATPase and its analysis by means of the theory of metabolic control (Kacser & Burns, 1973; Heinrich & Rapoport, 1974). Petronilli et al. (1988) used this analytical framework to conclude, from experiments with submitochondrial particles from beef heart, that the flux control coefficient of the mitochondrial F_oF_1-ATPase, for the overall process of oxidative phosphorylation, was equal to 1 (fully "rate limiting") under their experimental conditions. Such a conclusion was in agreement with previous independent observations by Herweijer et al. (1985). As shown in Appendix I, it can be easily deduced that, if this is the case, the experimentally determined Michaelis constants for ADP and P_i will correspond exactly to the real parameters K_m^{ADP} and $K_m^{P_i}$. The same conclusion does not apply, however, to the experimental value of V_{max}, which will be the consequence of a combined response by the overall pathway (Appendix I).

Table I: Effect of Partial Inhibition by Venturicidin on Kinetics of Oxidative Phosphorylation in *P. denitrificans*

[venturicidin] [μg·(mg of protein)$^{-1}$]	V_{max} [nmol·min^{-1}·(mg of protein)$^{-1}$]	K_m^{ADP} (μM)
(A) ADP as Variable Substrate[a]		
	904	8.1
0.07	694	8.0
0.18	431	8.2
[venturicidin] [μg·(mg of protein)$^{-1}$]	V_{max} [nmol·min^{-1}·(mg of protein)$^{-1}$]	$K_m^{P_i}$ (μM)
(B) P_i as Variable Substrate[b]		
	1970	341
0.09	1420	337
0.15	1040	348
0.31	590	344

[a] The rate of phosphorylation catalyzed by membrane vesicles (0.21 mg of protein·mL^{-1}) was measured as in Figure 1, except that venturicidin was added to the final concentration indicated, at least 3 min before respiration was started. The kinetic parameters were derived from the corresponding Hanes plots of [ADP]/v vs [ADP] (concentration range 2–90 μM). [b] The rate of phosphorylation catalyzed by membrane vesicles (0.08 mg of protein·mL^{-1}) was measured as in Figure 2, except that venturicidin was added at least 3 min before respiration was started. The concentration of ADP used was 270 μM. The kinetic parameters were obtained as before from the application of eq 1.

To investigate whether or not the same is true for the bacterial system under the experimental conditions used here, the effect on oxidative phosphorylation of the energy-transfer inhibitor venturicidin (Linnet & Beechey, 1979) was investigated. As previously reported (Ferguson & John, 1977), controls of the different states of respiration in the presence of venturicidin showed that the effect of the inhibitor on the kinetics of ATP synthesis is due exclusively to its action on the F_oF_1-ATPase (not shown). Venturicidin was found to behave as an apparently pure noncompetitive inhibitor, causing the expected decrease of the measured V_{max} but no detectable changes in K_m^{ADP} and $K_m^{P_i}$ (Table I). As shown in Appendix I, such a result can only be explained if the flux control coefficient of the F_oF_1-ATPase is equal to 1, in line with the findings by Petronilli et al. (1988). Otherwise, clear increases in K_m^{ADP} and $K_m^{P_i}$ should have been detected.

The noncovalent nature of the binding of venturicidin to the F_oF_1-ATPase (Linnet & Beechey, 1979) had to be taken into account, because it might allow modification of the affinity of the inhibitor for its binding site upon membrane energization (Herweijer et al., 1985), therefore compromising the kinetic analysis included here. In fact, such a change in the affinity for venturicidin when the membrane was energized was found in parallel titrations of ATP synthesis and ATP hydrolysis (Figure 3A). To be able to monitor the second reaction, the hydrolytic activity of the F_oF_1-ATPase was greatly activated by the presence of a high concentration of the anion sulfite (Pérez et al., 1986; Ballard, 1988) and measured in fully uncoupled conditions. It was found that inhibition by venturicidin was significantly stronger for ATP synthesis, suggesting a higher affinity for the inhibitor in phosphorylating conditions. As discussed in Appendix I, however, a positive dependence on Δp of the affinity for venturicidin is unable to account for the noncompetitive pattern of inhibition on ATP synthesis (Table I).

An additional set of venturidicin titrations for ATP synthesis was carried out with partial uncoupling by FCCP, or with respiration partially blocked by rotenone, and compared with a control titration in the absence of either effector (Figure 3B).

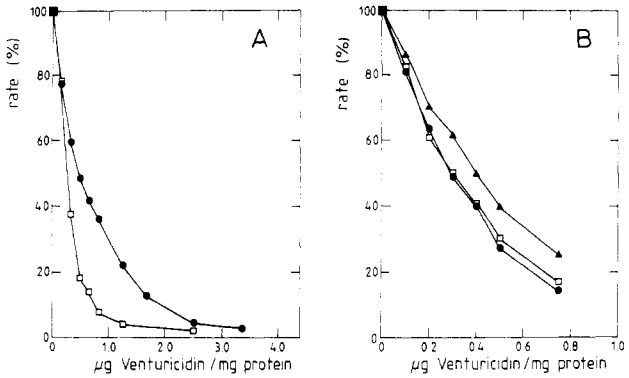

FIGURE 3: Titrations of the inhibition by venturicidin of the maximal rates of ATP synthesis/hydrolysis in *P. denitrificans*. (A) The rate of phosphorylation of membrane vesicles (0.12 mg of protein·mL^{-1}) was measured as in Figure 1, in the presence of 10 mM [^{32}P]P_i, 199 μM ADP, and increasing amounts of venturicidin (□). In parallel, the rate of hydrolysis was measured as described under Materials and Methods, in a total volume of 3 mL which also contained 100 mM K_2SO_3, 3 μM FCCP, and increasing amounts of venturicidin (●). The rates of synthesis and hydrolysis measured in the absence of venturicidin were 2790 nmol of ATP·min^{-1}·(mg of protein)$^{-1}$ and 3640 nmol of P_i·min^{-1}·(mg of protein)$^{-1}$, respectively. (B) The rate of phosphorylation catalyzed by membrane vesicles (0.3 mg of protein·mL^{-1}) was measured as in (A), in the presence of increasing amounts of venturicidin (●). In parallel titrations, rotenone [10 μg·(mg of protein)$^{-1}$] (□) or FCCP (1.5 μM) (▲) was also present. The rates measured in the absence of venturicidin were 2810 (●), 1190 (□), and 620 nmol of ATP·min^{-1}·(mg of protein)$^{-1}$ (▲), respectively.

It was found that the titrations with and without rotenone were virtually identical but sharper than the titration in the presence of FCCP. Given the fact that the rate of phosphorylation with no added venturicidin was significantly lower in the presence of FCCP than in the presence of rotenone, the discrepancy between the titrations with rotenone or FCCP present could, in principle, be explained by the expected differences in Δp. However, the same explanation does not account for the similarity of the titrations with and without rotenone (Figure 3B). This similarity implies not only that the affinity for venturicidin is unaffected by the drop in Δp due to the addition of rotenone (Parsonage, 1984) but also that the flux control coefficient of the F_oF_1-ATPase remains unchanged and equal to 1 (see Appendix I). Therefore, it is very likely that the increase in the affinity for venturicidin, due presumably to an increase in Δp, reaches a maximum point at a low value of Δp above which further increments in Δp are not followed by similar changes in affinity. It is important to emphasize that, whatever is the actual dependence on Δp of the affinity for the inhibitor, the conclusion presented here of a fully mechanistic significance for the measured K_m^{ADP} and $K_m^{P_i}$ remains unshaken. This is of direct relevance to the kinetic analysis presented in this paper.

Irreversibility of the F_oF_1-ATPase from P. denitrificans. To study the effect of product inhibition on the kinetics of ATP synthesis, the reaction must be conducted in the presence of significant amounts of ATP, without any interference from ATP-consuming processes. Membrane preparations from *P. denitrificans* have previously been shown to be suitable for such studies, because they catalyze very low rates of ATP hydrolysis (Ferguson et al., 1976; Harris et al., 1977). A detailed examination of this system showed that, while being capable of catalyzing very high rates of phosphorylation, rates of ATP hydrolysis were negligible (Table II). The basal rate observed in the absence of respiration was only marginally increased by the onset of respiration, and this increase was negated by addition of the uncoupler FCCP. Confirming previous observations (Ferguson, 1975; Harris et al., 1977), the basal rate

Table II: Analysis of Reversibility of F_oF_1-ATPase from *P. denitrificans*

	ATP hydrolysis[a]	ATP ⇌ P_i exchange[b]	ATP synthesis[c]
(A) no respiration	6.3		
(B) as in (A), +PK/PEP/K^+[d]	6.5		
(C) respiration[e]	18.9	160	2390
(D) as in (C), +FCCP (3 μM)[f]	6.3	0	16
(E) as in (A), +venturicidin [0.73 μg·(mg of protein)$^{-1}$][f]	6.5		

[a] The rates of ATP hydrolysis were measured as described under Materials and Methods with 0.56 mg of vesicle protein·mL^{-1} and are presented in units of nmol of P_i·min^{-1}(mg of protein)$^{-1}$. [b] The rates of ATP ⇌ P_i exchange were measured as described under Materials and Methods with 0.28 mg of vesicle protein·mL^{-1} and are shown in units of nmol of [γ-^{32}P]ATP·min^{-1}·(mg of protein)$^{-1}$. [c] The rates of ATP synthesis were measured in the presence of hexokinase and glucose as described under Materials and Methods with 0.28 mg of vesicle protein·mL^{-1}, 10 mM P_i, and 224 μM ADP and are given in units of nmol of ATP·min^{-1}·(mg of protein)$^{-1}$. [d] The reaction mixture also contained ~6 units·mL^{-1} pyruvate kinase (PK), 1.13 mM phosphoenolpyruvate (PEP), and 5 mM K_2SO_4. [e] Respiration was sustained by addition of 0.6 mM NAD^+, 1% (v/v) ethanol, and 0.1 mg of alcohol dehydrogenase·mL^{-1}. NAD^+ was added at least 1 min before addition of ATP (exchange) or ADP (synthesis). [f] FCCP and venturicidin were added as ethanolic solutions.

of hydrolysis did not seem to be due to the F_oF_1-ATPase, as indicated by the lack of effect by the specific inhibitor venturicidin. No increase was observed in the presence of pyruvate kinase and phosphoenolpyruvate, therefore indicating that the very low rate of ATP hydrolysis was not the result of any inhibitory effect by the ADP present in solution (Table II).

The presence of ATP could interfere with the incorporation of ^{32}P from [^{32}P]P_i into organic phosphate (used in this work to determine the rates of phosphorylation) due to an ATP ⇌ P_i exchange reaction. The corresponding control showed that this rate of exchange, although it is significantly higher than the rate of ATP hydrolysis, only reaches 7% of the rate of ATP synthesis when carried out in the presence of 10 mM ATP (Table II). In parallel to the rate of phosphorylation, the ATP ⇌ P_i exchange is completely abolished by uncoupler.

Coupling Conditions of Membrane Vesicles from P. denitrificans. The ability of membrane preparations from *P. denitrificans* to build up large phosphorylation potentials, ΔG_P, was investigated (Figure 4). The determination of ΔG_P by measuring the concentrations of P_i, ADP, and ATP (once thermodynamic equilibrium is reached) was avoided because of the inevitable hydrolysis of small proportions of the ATP present that is always produced when the reaction mixture is quenched by addition of perchloric acid (Eilermann & Slater, 1970; Petronilli et al., 1986; Lemasters & Fleishman, 1987). Instead, the reaction of ATP synthesis was monitored by following the incorporation of ^{32}P from [^{32}P]P_i into ATP in reaction mixtures containing low initial concentrations of P_i and ADP (Figure 4). The final concentrations of the latter were obtained by difference. This procedure allowed the concentrations of the three ligands, [^{32}P]P_i, ADP, and [γ-^{32}P]ATP, to be monitored at many time points after the attainment of thermodynamic equilibrium, therefore making the determination of ΔG_P simple and precise. In normal conditions, values of ΔG_P around 61 kJ/mol were attained (Figure 4), somewhat higher than those reported previously for this system (McCarthy & Ferguson, 1983). This means that, in the presence of 10 mM P_i, ratios of [ATP]/[ADP] as high as 2000 can be expected, thus allowing for significant amounts of ATP to be present during the phosphorylating reaction without suffering thermodynamic constraints. Figure 4 also

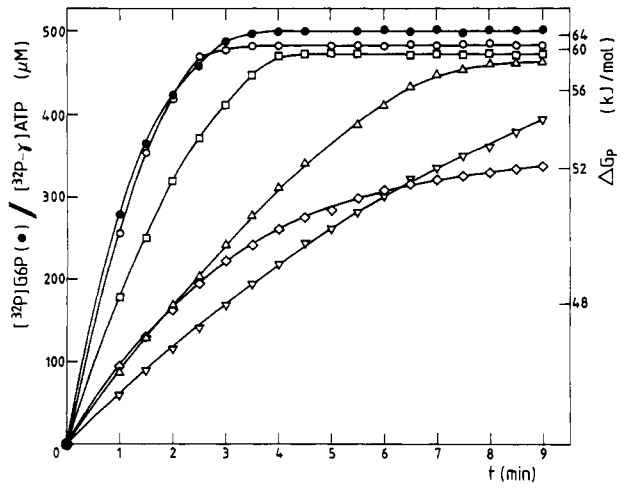

FIGURE 4: Phosphorylation potential ΔG_P generated by membrane vesicles from *P. denitrificans*. The incorporation of ^{32}P into organic phosphate was monitored as described under Materials and Methods, for reaction mixtures containing vesicles (0.19 mg of protein·mL^{-1}) in the presence of initial concentrations of P_i (500 μM) and ADP (630 μM). In one case only (●), hexokinase and glucose were also present. Other effectors were added: none (○), rotenone [5.3 μg·(mg of protein)$^{-1}$] (□), potassium cyanide (15 μM) (△), FCCP (0.8 μM) (◇), and myxothiazol [0.32 μg·(mg of protein)$^{-1}$ (▽). ΔG_P was determined from the concentrations at equilibrium of [^{32}P]P_i, ADP, and [γ-^{32}P]ATP with $\Delta G_P = \Delta G^{\circ\prime} + RT \ln ([ATP]/[ADP][P_i])$, where $\Delta G^{\circ\prime}$ was given the value of 30.1 kJ·mol^{-1} (Rosing & Slater, 1972). The total concentration of ATP was corrected for the minor amount of ATP initially present as contamination of the ADP used.

shows the effects on ΔG_P of partial inhibition of the respiratory chain and partial uncoupling. An important independent control (not shown) indicated that membrane preparations from *P. denitrificans* have no adenylate kinase activity.

Determination of the Type and Extent of Product Inhibition. The effect of product inhibition on the phosphorylating reaction was first analyzed from the progress curve obtained in the presence of a limited concentration of ADP (saturating [P_i]) and the absence of hexokinase and glucose (Figure 5A). Given the high value of ΔG_P attained by this system, a virtually complete consumption of the added ADP was observed, with the progress curve unaffected by the negligible reverse reaction. The apparent kinetic parameters associated with the progress curve ($^{app}K_m^{ADP}$ and $^{app}V_{max}$) were extracted from the application of eq 2 (see Materials and Methods), which produced a linear plot of $t/\ln(b_o/b)$ vs $(b_o - b)/\ln(b_o/b)$, where $b \equiv$ [ADP] (Figure 5B).

In order to compare the apparent parameters $^{app}K_m^{ADP}$ and $^{app}V_{max}$ with those obtained from initial rate measurements, additional measurements of initial rates in the presence of hexokinase, glucose, and a range of ADP concentrations were made (Figure 5B). The comparison of the corresponding representation of eq 2 (for the progress curve) with the Hanes plot of [ADP]/v vs [ADP] (for the initial rates) gave an indication of the extent of product inhibition (Figure 5B). The two representations were apparently parallel ($^{app}V_{max} \simeq V_{max}$) and only differed slightly in their intersection with the x axis ($^{app}K_m^{ADP} > K_m^{ADP}$). Such a result is, in principle, similar to that previously observed in chloroplasts (Franek & Strotmann, 1981) and compatible with a weak inhibition by product of a purely competitive nature.

However, the experiment shown in Figure 5 was only able to reveal the inhibitory effect produced by a rather small concentration of ATP, generated by the phosphorylating reaction itself. In order to determine accurately the type of product inhibition and the apparent affinity of the enzyme for ATP under these conditions, ATP synthesis had to be measured in the presence of much larger concentrations of the nucleotide. A preliminary control showed the need to set the total concentration of Mg^{2+} (5 mM) in excess of that of ATP, in order to maintain the levels of free Mg^{2+} required for an optimal phosphorylating activity (not shown). Any complications from ATP hydrolysis or ATP ⇌ P_i exchange, or from limiting values of ΔG_P, had been ruled out (Table II and Figure 4).

The simultaneous addition of a limited concentration of ADP and millimolar concentrations of ATP resulted in a clear

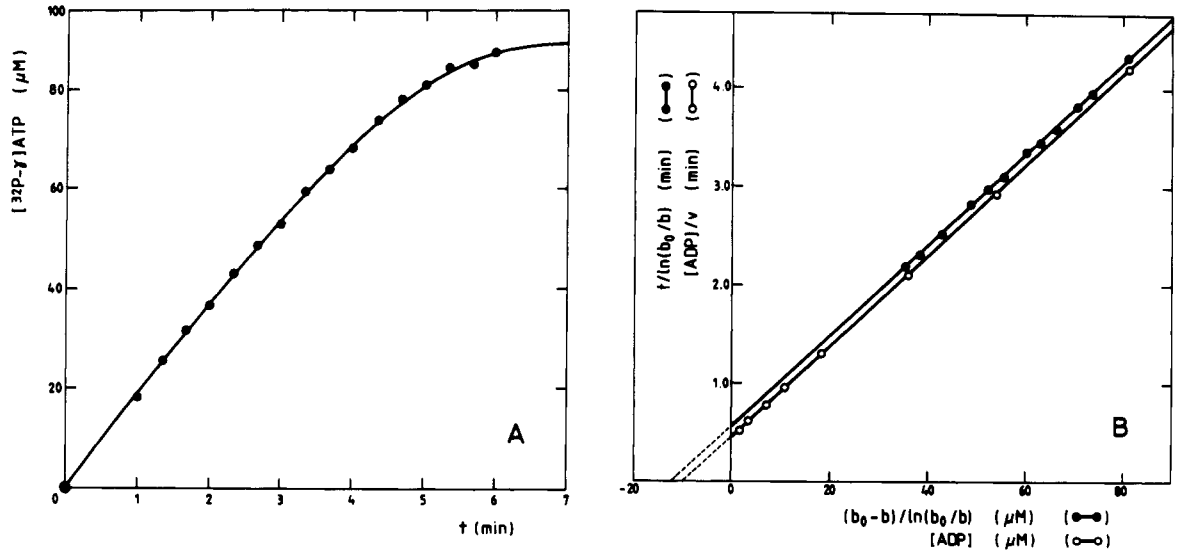

FIGURE 5: Initial characterization of the extent of product inhibition during ATP synthesis catalyzed by membrane vesicles from *P. denitrificans*. (A) The progress curve of the formation of [γ-^{32}P]ATP from 10 mM [^{32}P]P_i and 90 μM ADP catalyzed by membrane vesicles (13.6 μg of protein·mL^{-1}) was obtained as described under Materials and Methods. (B) The data from the progress curve were represented according to eq 2 (●) where $b \equiv$ [ADP] (see Materials and Methods). In the same experiment, initial rates of phosphorylation were also measured in the presence of hexokinase and glucose, 10 mM [^{32}P]P_i, and a range of ADP concentrations, as described in Figure 1. For direct comparison with the plot of the progress curve, the same total volume (4 mL) and amount of vesicles were used to measure initial rates. Aliquots of the same volume (100 μL) were withdrawn to determine the incorporation of ^{32}P into [^{32}P]G6P. The corresponding Hanes plot of [ADP]/v vs [ADP] is shown (○). The kinetic parameters derived were V_{max} ($\simeq ^{app}V_{max}$) = 1540 nmol of ATP·min^{-1}·(mg of protein)$^{-1}$, $^{app}K_m^{ADP}$ = 11.7 μM (progress plot), and K_m^{ADP} = 10.0 μM (initial rates).

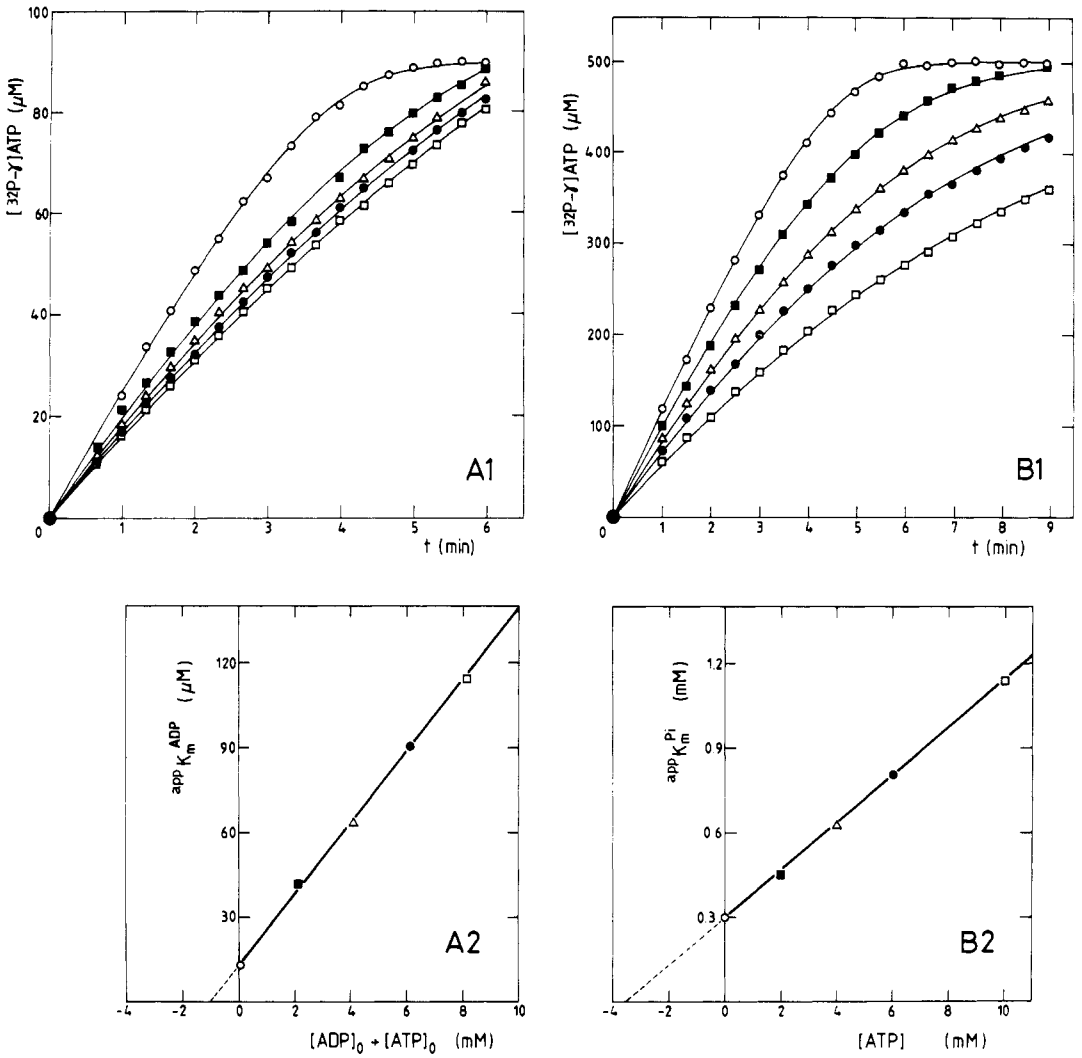

FIGURE 6: Type and extent of product inhibition and order of binding of ADP and P_i. (A1) Progress curves of the formation of [γ-^{32}P]ATP from 10 mM [^{32}P]P_i and limited concentrations of ADP were obtained as in Figure 5, though in the presence of a range of initial concentrations of ATP. With the membrane vesicles (12.8 μg of protein·mL^{-1}), the following concentrations of nucleotides were initially added: ADP at 89.7 (○), 103.3 (■), 116.9 (△), 130.5 (●), or 144.1 μM (□); ATP at 0 (○), 2.0 (■), 4.0 (△), 6.0 (●), or 8.0 mM (□). The progress curves were fitted to eq 3 by computer (see Materials and Methods). The reaction carried out in the absence of added ATP (○) provided the corresponding $^{app}K_m^{ADP}$ and the fixed value of $^{app}V_{max}$ [2280 nmol of ATP·min^{-1}·(mg of protein)$^{-1}$], which was applied to the remaining progress curves to obtain the related $^{app}K_m^{ADP}$ (see text). The solid lines correspond to the computer-fitted solutions. (A2) The derived values of $^{app}K_m^{ADP}$ were plotted versus $[ADP]_o + [ATP]_o$ (initial concentrations) according to eq 6 (see text). The intersection of the resulting linear plot with the x axis gives the value of $^{app}K_i^{ATP}$ (1.0 mM) (see text). (B1) In the same experiment, progress curves of the formation of [γ-^{32}P]ATP from 500 μM [^{32}P]NaH_2PO_4 and 1.79 mM ADP, catalyzed by membrane vesicles (89 μg of protein·mL^{-1}) in the presence of a millimolar range of initial concentrations of ATP, were also obtained. As in Figure 2, the reaction mixtures were buffered with 21 mM Tris/HCl (pH 7.3). The ATP range was as follows: 0 (○), 2.0 (■), 4.0 (△), 6.0 (●), or 10.0 mM (□). The data were processed as in (A1) considering P_i as the only variable substrate (see text); this simplification produced a pseudoapparent maximal rate given by $^{app}V_{max}$ = 1560 nmol of ATP·min^{-1}·(mg of protein)$^{-1}$ (see also Table V). (B2) The data from (B1) and Table V were used to construct the plot of $^{app}K_m^{P_i}$ vs [ATP]. The intercept with the x axis gives $^{app}K_i^{ATP}$ = 3.4 mM. See text for more details.

decrease in the rate of phosphorylation due to product inhibition (Figure 6, panel A1). To analyze the data, a computer-fitting program based on eq 3 (see Materials and Methods) was required. As pure competitive product inhibition was assumed (see below), the reaction in the absence of added ATP was used to extract the values of $^{app}V_{max}$ and $^{app}K_m^{ADP}$ associated with that reaction. This value of $^{app}V_{max}$ was fixed and applied to the remaining reactions, in order to obtain the corresponding values of $^{app}K_m^{ADP}$ (Figure 6, panel A1). The solid lines in the figure correspond to the computer-fitted solutions.

The assumption of pure competitive product inhibition, taking the F_oF_1-ATPase as a monosubstrate enzyme (saturating P_i), produces the following rate equation:

$$v = dp/dt = \frac{V_{max}(b_o - p)}{K_m^B[1 + (p + p_o)/K_i^P] + (b_o - p)} \quad (4)$$

where $b \equiv [ADP]$, $p \equiv [ATP]$, and $b_o = b + p$; p represents the concentration of the ATP produced in the phosphorylating reaction; and p_o represents the concentration of ATP initially added to the reaction mixture (0–8 mM in Figure 6, panel A1). In eq 4, K_m^B corresponds to the Michaelis constant for ADP; K_i^P is the constant of pure competitive inhibition for ATP. Equation 4 can be integrated in the interval $(0, t) \rightarrow (0, p)$ to produce an equation identical with eq 2 with the apparent parameters $^{app}K_m^B$ and $^{app}V_{max}$ given by

$$^{app}V_{max} = V_{max}/(1 - K_m^B/K_i^P) \quad (5)$$

$$^{app}K_m^B = (K_m^BK_i^P)/(K_i^P - K_m^B) + [K_m^B/(K_i^P - K_m^B)](b_o + p_o) \quad (6)$$

In pure competitive inhibition, only $^{app}K_m^B$ is affected by the total concentration of ATP present in the reaction mixture so eq 6 can be used to construct the graphical plot of $^{app}K_m^B$ vs

$b_o + p_o$, producing a linear dependence (Figure 6, panel A2). The intersection with the x axis provides a direct reading for the value of K_i^P (1.0 mM in this experiment). Only pure competitive product inhibition is compatible with the linear plot and the satisfactory fitting of the progress curves of Figure 6, panel A1, with eq 3 and a fixed value for ${}^{app}V_{max}$. It is easy to show that any other type of inhibition would have generated a significantly nonlinear plot of ${}^{app}K_m^{ADP}$ vs $b_o + p_o$ (not shown). Thus, the previous assumption is confirmed.

F_oF_1-ATPase as a Two-Substrate Enzyme: Simultaneous Determination of the Order of Binding for ADP and P_i and of the Real Affinity for ATP. The analysis of progress curves and product inhibition presented in eq 2–6 assumes that the F_oF_1-ATPase operates as a monosubstrate enzyme, with ADP as the only variable substrate. Although this simplification is appropriate for experiments carried out in the presence of saturating concentrations of P_i (Figures 5 and 6A), it must not be forgotten that, in any two-substrate enzyme, the extent of pure competitive product inhibition depends directly on the degree of saturation of the enzyme with either one or both substrates (Rudolph, 1979; Cornish-Bowden, 1981). This implies that the value of K_i^{ATP} extracted from Figure 6, panel A2, can only be considered an apparent inhibition constant for ATP, which will be related to the real one (also the real dissociation constant for the binding of ATP to the active site) in a way that is a function of the order of binding for the two substrates (see Appendix II).

To determine the real affinity for ATP in the experiment shown in Figure 6 and, simultaneously, the order of binding for ADP and P_i, progress curves were also monitored for reactions where, together with a millimolar range of ATP concentrations, a limited concentration of P_i was initially present, in addition to a saturating concentration of ADP (Figure 6, panel B1). The analysis of these progress curves could not be done as before for two reasons: (i) The decreases in the concentration of ADP during the reactions were significant, and simplification to rate equations for a monosubstrate enzyme could not, in principle, be carried out. (ii) Control experiments showed that high concentrations of ADP produce pure competitive inhibition on the binding of P_i (see Table V). This effect was analogous to that previously reported for photophosphorylation in chloroplasts (Selman & Selman-Reimer, 1981). The value extracted for the associated inhibition constant was $K_i^{B'} = 2.6$ mM, where B ≡ ADP (Appendix II). This meant that the continuous consumption of ADP during the reactions shown in Figure 6, panel B1, was high enough to produce a progressive and significant increase in the apparent affinity for P_i, therefore making the analysis more complicated.

These limitations were circumvented by extrapolation to the initial rates from the progress curves of Figure 6, panel B1. The extrapolation was carried out by means of computer-aided fitting of the data to eq 3 as before. This was possible because the progress curves, despite the complications described, followed a "pseudo-monosubstrate" behavior which satisfied eq 3 surprisingly well (solid lines in Figure 6, panel B1). As detailed in Appendix II (see also Table V), the combination of these extrapolations with an independent determination of the real value of V_{max} resulted in a value of ${}^{app}K_m^{P_i}$ for each [ATP] used and allowed the construction of the ensuing plot of ${}^{app}K_m^{P_i}$ vs [ATP], which was linear (Figure 6, panel B2). The intersection with the x axis provided a direct reading of the apparent constant of inhibition for ATP, ${}^{app}K_i^{ATP} = 3.4$ mM (Appendix II).

Table III: Determination of K_i^{ATP} as a Function of the Order of Binding of ADP and P_i[a]

order of binding	K_i^{ATP} (eq used)[b]	
	${}^{app}K_m^B$ vs $b_o + p_o$[c]	${}^{app}K_m^A$ vs p_o[d]
(1) random	17.4 μM (eq A15)	14.0 μM (eq A22)
(2) compulsory (ADP first)	1.0 mM (eq A18)	14.0 μM (eq A23)
(3) compulsory (P_i first)	≃17.4 μM (eq A20[e])	2.0 mM (eq A24)

[a] This analysis corresponds to the data obtained from the experiment shown in Figure 6. For the calculations K_m^{ADP} ($=K_i^{ADP} = 12.5$ μM) was taken from the intersection with the y axis of the plot of ${}^{app}K_m^B$ vs $b_o + p_o$ (Figure 6, panel A2). $K_m^{P_i}$ ($=K_i^{P_i} = 175$ μM) and $K_i^{B'}$ (2.6 mM) were taken from the experiment shown in Table V, performed with the same vesicle preparation used in the experiment of Figure 6 only 24 h before. [b] The equations used to determine K_i^{ATP} are indicated in brackets. They are all given in Appendix II. [c] From Figure 6, panel A2, ${}^{app}K_i^{ATP} = 1.0$ mM. [d] From Figure 6, panel B2, ${}^{app}K_i^{ATP} = 3.4$ mM. [e] As indicated in Appendix II, eq A20 gives a nonlinear plot of ${}^{app}K_m^B$ vs $b_o + p_o$ if product inhibition is detectable. For the purpose of comparison, K_i^{ATP} was determined by approximation, assuming that eq A20 is linear, in which case eq A15 is again applicable.

The values of ${}^{app}K_i^{ATP}$ extracted from Figure 6, panels A2 and B2, are only apparent and cannot be considered a measure of the real affinity of the active site for ATP until the order of binding for ADP and P_i is determined. The three main possibilities were examined: (1) random order of binding for ADP and P_i; (ii) compulsory order of binding, with ADP entering the active site first; (iii) compulsory order of binding, with P_i first. The corresponding dependence of ${}^{app}K_i^{ATP}$ on (a) the real constant K_i^{ATP} and on (b) the degree of occupancy by ADP and/or P_i was determined for all three cases (see Appendix II). Table III shows the calculated values of K_i^{ATP} which result for the three possibilities from the plots of either ${}^{app}K_m^{ADP}$ vs $[ADP]_o + [ATP]_o$ (Figure 6, panel A2) or ${}^{app}K_m^{P_i}$ vs [ATP] (Figure 6, panel B2). It is obvious that only the true order of binding can provide a solution for K_i^{ATP} which is identical for both sets of data. The analysis shows very clearly that a random order of binding for ADP and P_i is the only one compatible with the extent of product inhibition found in both cases. The results indicate that the real inhibition constant K_i^{ATP} and, therefore, the real dissociation constant for the binding of ATP to the active site have a value (around 15 μM) significantly lower than the apparent ones (in a millimolar range).

The conclusion derived from the analysis presented in Table III implies that, within a more qualitative framework, the extent of competitive inhibition by ATP on the binding of one of the substrates is inversely affected by the extent of saturation of the binding of the other substrate. This was experimentally confirmed for the binding of ADP in the presence of a fixed concentration of ATP and two high but different concentrations of P_i (Figure 7); when $[P_i]$ was reduced from 10 to 4 mM, the rate of phosphorylation was unaffected throughout the progress curve when no ATP was initially present, though the extent of inhibition produced by 4 mM ATP was significantly increased. The lower concentration of P_i was still high enough to avoid thermodynamic restrictions on the reaction, indicating that the effect of the added ATP was only kinetic.

Kinetics of ATP Synthesis at Very Low Concentrations of ADP. Figure 1 showed that only a single Michaelis constant for ADP could be detected when initial rates of phosphorylation were measured for a wide range of concentrations ([ADP] = 2–2240 μM). This is somewhat surprising if the binding change mechanism proposed for the F_oF_1-ATPase is taken into consideration [e.g., Gresser et al. (1982)]. Indeed, Stroop and Boyer (1985) first reported the presence of two very different Michaelis constants for ADP, observed when

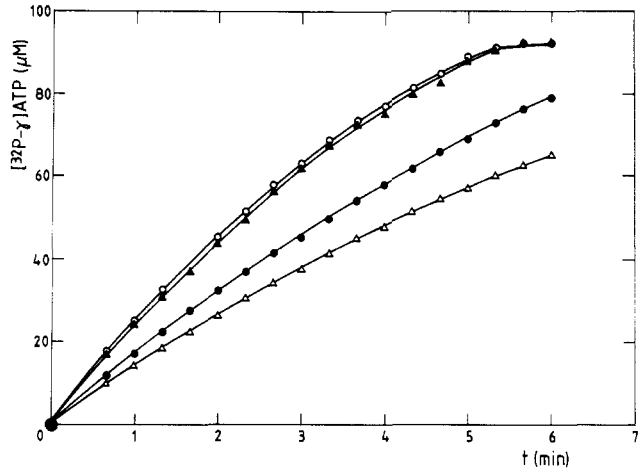

FIGURE 7: Product inhibition of ADP binding at two saturating but different concentrations of P_i. Progress curves of the formation of [γ-^{32}P]ATP from a limited concentration of ADP and two different but saturating concentrations of [^{32}P]P_i, in the presence or absence of an initial millimolar concentration of ATP, were obtained as in Figure 6. With the membrane vesicles (13.6 μg of protein·mL^{-1}), the following concentrations of substrates and product were initially added: [^{32}P]NaH_2PO_4 at 10.0 (○, ●) or 4.0 mM (▲, △); ADP at 90 (○, ▲) or 114 μM (●, △); ATP at 0 (○, △) or 4.0 mM (●, △). The reaction mixtures were buffered with 21 mM Tris/HCl (pH 7.3).

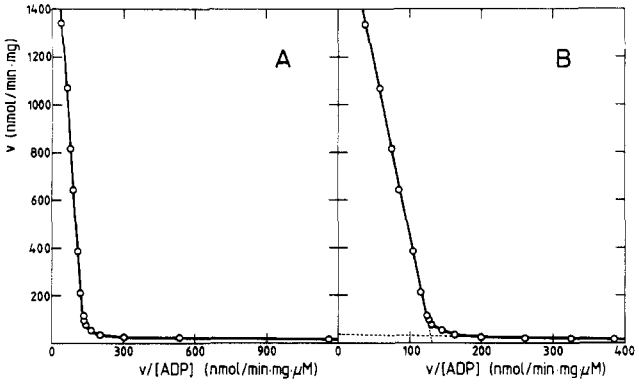

FIGURE 8: Kinetics of ATP synthesis at very low concentrations of ADP. The rate of phosphorylation catalyzed by membrane vesicles of *P. denitrificans* (0.49 mg of protein·mL^{-1}) was measured in the presence of 10 mM [^{32}P]P_i, hexokinase/glucose, and a wide range of concentrations of ADP (0.02–36 μM), as in Figure 1. (A) Eadie–Hofstee plot of v vs v/[ADP] of the original data. The additional rate of phosphorylation obtained in the absence of any added ADP [v = 17.8 nmol of ATP·min^{-1}·(mg of protein)$^{-1}$] is not shown. (B) Final Eadie–Hofstee plot obtained after correction of [ADP] with the estimated concentration of endogenous ADP (see text for explanation). The kinetic parameters derived from this plot are $K_{m,1}^{ADP}$ = 51 nM and $V_{max,1}$ = 37.5 nmol of ATP·min^{-1}·(mg of protein)$^{-1}$ for the low ADP range, while $K_{m,2}^{ADP}$ = 13.3 μM and $V_{max,2}$ = 1840 nmol of ATP·min^{-1}·(mg of protein)$^{-1}$ for the high ADP range.

studying photophosphorylation in chloroplasts. Similar findings have also been reported for oxidative phosphorylation by beef heart submitochondrial particles (Matsuno-Yagi & Hatefi, 1985, 1986; Hekman et al., 1988).

The possibility of an additional K_m^{ADP} at very low concentrations of ADP, undetected in previous experiments, was investigated by measuring the rate of phosphorylation in the presence of added amounts of ADP within the range 0.02–36 μM. The results were used to construct the corresponding Eadie–Hofstee plot of v vs v/[ADP] (Figure 8A). It can be seen that, while the concentrations of ADP between 1.8 and 36 μM generate a linear plot in agreement with the Michaelian behavior seen before, the smaller concentrations of added ADP are associated with rates that deviate progressively toward greater values than those predicted from the parameters K_m^{ADP} and V_{max} obtained with the highest range of concentrations (Figure 8A). The deviation is such that a measurable rate of phosphorylation was detected even in the complete absence of added ADP (not shown in Figure 8A). A control reaction, carried out in the absence of added ADP and hexokinase, failed to generate incorporation of ^{32}P into organic phosphate, therefore confirming that the former was due to ATP synthesis. The "endogenous" ADP present in the reaction mixtures could have been present in the membrane vesicles themselves as a consequence of the preparation procedure (John, 1977) or present in the commercial hexokinase used.

Table IV: Summary of Kinetic Parameters Associated with ATP Synthesis by Membrane Vesicles from *P. denitrificans*

(A) Enzymatic Cycle with High Affinity and Low Turnover	
$K_{m,1}^{ADP}$ (nM)	≃50
$K_{m,1}^{P_i}$	nd[a]
order of binding	nd
$V_{max,1}$	≃0.02$V_{max,2}$
(B) Enzymatic Cycle with Low Affinity and High Turnover	
$K_{m,2}^{ADP}$ (=$K_{i,2}^{ADP}$) (μM)	11 ± 1[b]
$K_{m,2}^{P_i}$ (=$K_{i,2}^{P_i}$) (μM)	224 ± 18[c]
order of binding	random
K_i^{ATP} (μM)	16 ± 1[d,e]
$V_{max,2}$ [μmol of ATP·min^{-1}·(mg of protein)$^{-1}$]	0.7–2.7[f]

[a] nd = not determined. [b] Given as the mean ±SEM obtained from 15 different membrane vesicle preparations. [c] Given as the mean ± SEM obtained from 13 different membrane vesicle preparations. [d] Given as the mean ± SEM obtained from five different membrane vesicle preparations. [e] Pure competitive product inhibition. [f] Range obtained from more than 40 different membrane vesicle preparations; a mean value is not given as explained under Results.

Figure 8A clearly shows the existence of two very different and well-defined Michaelis constants for ADP, linked to very different maximal rates. The determination of the smaller pair, $K_{m,1}^{ADP}$ and $V_{max,1}$ was hindered by the unknown amount of ADP present in the reaction mixtures when no extra substrate is added. Nevertheless, an estimate of these parameters could be obtained by means of an iterating protocol: this derived the value of the endogenous concentration of ADP from a linear regression (v vs [ADP]/v) applied to the three lower points of Figure 8A and used this value to obtain, in turn, a new linear regression after correction for [ADP]. The resulting set of iterations converged to an optimal linear regression (shown in Figure 8B), which gave the final estimates of the low $V_{max,1}$ [=37.5 nmol of ATP·min^{-1}·(mg of protein)$^{-1}$] and $K_{m,1}^{ADP}$ (=51 nM), as well as the endogenous concentration of ADP (=46 nM). Although these figures are only estimates of the real values, they strongly suggest the existence of an active site in the F_oF_1-ATPase with very high affinity for ADP but very low catalytic capacity. This finding is in line with the binding change mechanism and resembles very closely the results reported by Stroop and Boyer (1985) for chloroplasts.

Discussion

The studies of oxidative phosphorylation in *P. denitrificans* shown in this paper represent a characterization of the basic features of the mechanism of ATP synthesis at the active site(s) of the F_oF_1-ATPase. A summary of the results obtained is presented in Table IV. These results indicate the presence of two well-defined enzymatic cycles, of very different ligand affinities and catalytic capacities, which appear compatible with the binding change mechanism proposed for this enzyme [e.g., Kayalar et al. (1977) and Gresser et al. (1982); for review, see Cross (1981), Senior (1988), and Boyer (1989)].

To assist the discussion of the results summarized in Table IV, a very elementary representation of the putative mechanism of ATP synthesis at the active site(s) is presented in

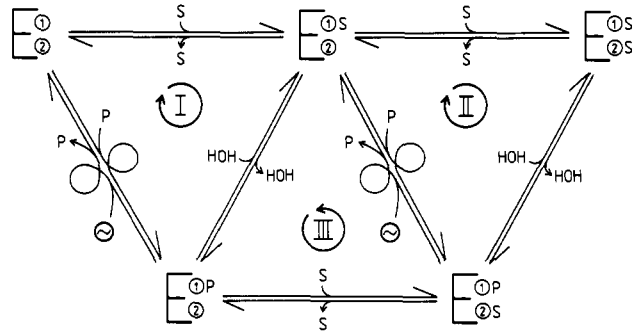

FIGURE 9: ATP synthesis by F_oF_1-ATPases from *P. denitrificans* according to the binding change mechanism. A minimal scheme of two alternating active sites is presented. See Discussion for references and further explanation. For simplicity, symbols used are S ≡ ADP + P_i and P ≡ ATP. Site 1 represents the active site with highest affinity for S, where the reversible interconversion of S ⇌ P takes place. Site 2 represents an active site with lower affinity for S and the one which binds P. Two extreme catalytic cycles are deduced: cycle I of high affinity and low turnover, when S levels are enough to occupy only site 1; cycle II of low affinity and high turnover, when higher S levels allow binding to site 2. It is assumed that the binding of S to site 2 promotes a faster interconversion of S ⇌ P in site 1 and a faster release of P. In the presence of intermediate levels of S, a third catalytic cycle III, of low affinity and intermediate turnover, can also occur if the interconversion S ⇌ P in site 1 takes place before binding of S to site 2. Energy input is used to induce the simultaneous and concerted conformational changes which promote the release of P. These are 1(P) → 2 and 2 → 1 for cycle I and 1(P) → 2 and 2(S) → 1(S) for cycles II and III.

Figure 9, in accordance with the binding change mechanism. A scheme of only two alternating sites is described, compatible with the results presented in this paper; the different (but interconverting) sites possess affinities for substrate(s) and product which are also very different. The main feature of the model is that the major input of energy into the catalytic cycle is used to promote the release of tightly bound ATP from the active site (Boyer et al., 1973). This release of product is induced by a simultaneous and concerted conformational change of the active sites, which interchanges their catalytic and binding properties. According to Boyer and co-workers [e.g., Hackney and Boyer (1978) and Hackney et al. (1979)], the number of reversals at the active site prior to the release of ATP will be much greater at low substrate concentrations (catalytic cycle I in Figure 9) than at higher ones (catalytic cycle II). More details of the scheme are included in the legend to Figure 9.

A main conclusion of the study reported here is that, during oxidative phosphorylation in *P. denitrificans*, ATP produces pure competitive product inhibition due to its binding at the active site of the F_oF_1-ATPase (Figure 6), as previously reported during photophosphorylation in chloroplasts (Franek & Strotmann, 1981). However, the real affinity of the active site for ATP during net ATP synthesis (16 μM, Table IV) is significantly higher than the apparent one measured in chloroplasts [$^{app}K_i^{ATP}$ = 4.4 mM in Franek and Strotmann (1981)]. This is readily explained by the random order of binding of the substrates, ADP and P_i, at the active site (Table III); binding of only one substrate, either ADP or P_i, is sufficient to hinder the binding of ATP. For this reason, the apparent inhibition constants measured for ATP in the presence of saturating concentrations of either substrate will be significantly higher than the real one (Table IV). This is also very likely to be the case for photophosphorylation in chloroplasts, since Magnuson and McCarty (1976) measured the affinity for ATP at the active site of the F_oF_1-ATPase upon illumination, as given by a dissociation constant in the micromolar range (K_d^{ATP} = 7 μM), determined from the exchange of nucleotide between the enzyme and the medium (Magnuson & McCarty, 1976).

The thermodynamic significance of the real affinity for ATP during net ATP synthesis deserves consideration. Assuming a very high affinity for ATP at the active site of the enzyme (site 1 in Figure 9), as initially reported for both isolated and membrane-bound mitochondrial F_1 (K_d^{ATP} = 10^{-12} M; Grubmeyer et al., 1982; Penefsky, 1985a), a very large change in the dissociation constant is to be expected in order to avoid product inhibition during ATP synthesis; such a requirement is a direct consequence of the millimolar concentration of ATP generally observed in mitochondria, chloroplasts, or bacteria (Mathews, 1972; Senior, 1988). As discussed by Grubmeyer et al. (1982), at least in mitochondria this could exceed the energy available from respiration (Brand & Lehninger, 1977). It is for this reason that the evolutionary selection of a random order of binding for ADP and P_i (Table III) makes "biological sense". The presence of high concentrations of only one substrate (either ADP or P_i) is then sufficient to block the access of ATP to the active site(s); this allows the affinity for the nucleotide to be higher than previously thought (K_i^{ATP} in a micromolar range compared to $^{app}K_i^{ATP}$ in a millimolar range) and, therefore, significantly reduces the energy demands of the phosphorylating reaction.

As summarized in Table IV, a second very low K_m^{ADP} is also observed, associated with an equally low V_{max} (Figure 8). As previously mentioned, this result closely resembles observations in chloroplasts (Stroop & Boyer, 1985). Figure 9 explains these findings; catalytic cycle I corresponds to the binding of ADP and P_i to the site of higher affinity for substrate(s) and product (site 1), which accounts for the low K_m^{ADP} and V_{max} (presumably there is also a low $K_m^{P_i}$, not determined here). In the presence of higher concentrations of ADP and/or P_i, the substrates can bind to the second site (site 2), therefore entering catalytic cycle II, which accounts for the high K_m^{ADP}, $K_m^{P_i}$, and V_{max}. In both cycles I and II the major energy input is assumed to occur at the step of conformational change induced ATP release, while the previous step of interconversion, ADP + P_i ⇌ ATP + H_2O, takes place reversibly at the active site of high affinity (site 1), without requiring energy [e.g., Rosing et al. (1977) and Choate et al. (1979)]. In the case of *P. denitrificans*, the extreme differences in affinity and catalytic capacity between cycles I and II (Figure 8) indicate clearly that, for most purposes, away from a submicromolar range of ADP concentrations the F_oF_1-ATPase can be taken as a simple Michaelian enzyme operating exclusively through cycle II.

In the scheme of Figure 9 with only two alternating active sites, in agreement with the pure competitive product inhibition for ATP synthesis observed experimentally [this paper; also Franek and Strotmann (1981)], substrates and product bind to the same site of low affinity (site 2). The possibility of a binding change mechanism involving three alternating active sites (Gresser et al., 1982) can also account for these results. However, some restrictions have to be imposed on a three-site model; the detection of only two well-defined Michaelis constants for ADP (Stroop & Boyer, 1985; this paper) implies that either the binding of substrate(s) to the second and third sites shows identical affinities and turnover rates or the third site possesses a negligible affinity for substrate(s). Although the latter option would predict mixed inhibition by ATP (not shown) instead of pure competitive inhibition, the former one would be compatible with this type of inhibition.

Figure 9 also illustrates that, whatever the degree of occupancy by substrate(s) of the different catalytic sites, all of them

Table V: Competitive Inhibition by ADP of the Binding of P_i

	[ADP] (mM)	V_{max} [nmol of ATP·min^{-1}·(mg of protein)$^{-1}$]	$^{app}K_m^{P_i}$ (μM)
I[a]	0.45	2260	210
	1.79	2270	300
II[b]	1.79 (without HK)	1560[c]	82[c]
	1.79 (with HK)	2160	304

[a] Progress curves of reactions carried out in the presence of 0.5 mM [^{32}P]P_i and hexokinase/glucose were obtained as in Figure 2, corresponding to two different concentrations of added ADP. The associated parameters V_{max} and $^{app}K_m^{P_i}$ were derived and used to determine the inhibition constant K_i^{ADP} (2.6 mM) (see text). The real value of $K_m^{P_i}$ (175 μM) was also extracted from the same calculations. [b] As part of the experiment shown in Figure 6, panel B1, an additional reaction was carried out in the presence of 0.5 mM [^{32}P]P_i and 1.79 mM ADP, with no added ATP, but with hexokinase (HK) and glucose. This reaction and the reaction of Figure 6, panel B1, carried out without added ATP or hexokinase, were plotted according to eq 1, and the associated parameters V_{max} and $^{app}K_m^{P_i}$ were obtained. [c] Pseudoapparent parameters. See text for explanation.

participate simultaneously in the mechanism of the enzyme. This is an essential feature of the binding change mechanism [e.g., Hackney et al. (1979)] and argues against the interpretation offered by Hekman et al. (1988) for the reported curvilinear kinetics of oxidative phosphorylation in beef heart submitochondrial particles (Matsuno-Yagi & Hatefi, 1985, 1986): (i) The transition between cycles I and II ("low" and "high" kinetic modes, according to those authors) is only a consequence of increasing substrate concentrations and not of a proposed modulation by energy input (Matsuno-Yagi & Hatefi, 1986). In fact, variations in energy input produce a concomitant change in the kinetic parameters of the system by directly affecting the rate constant for the release of ATP (Hackney et al., 1979). (ii) It is not strictly correct to analyze the variations in the rates of oxidative phosphorylation due to changes in substrate concentrations as a composite of two (or three) additive sets of pairs of K_m^{ADP} ($K_m^{P_i}$) and V_{max} (Matsuno-Yagi & Hatefi, 1985, 1986; Hekman et al., 1988). As can be deduced from Figure 9, as soon as the substrate concentration is high enough to enter cycle II, then slower cycle I becomes redundant; i.e., the two cycles are mutually exclusive, not additive.

In the presence of intermediate substrate concentrations a new feature becomes relevant. The conversion ADP + $P_i \rightleftharpoons$ ATP + H_2O in site 1 can occur before the binding of a new substrate(s) to site 2, generating in this way an additional third cycle, III (Figure 9), with kinetic characteristics which are intermediate between those of cycles I and II. This cycle III can produce, in turn, an apparent third pair of parameters, K_m^{ADP} ($K_m^{P_i}$) and V_{max}, similar to that reported by Hekman et al. (1988). Also, the coexistence of the three catalytic cycles I–III could possibly account for the changes in the distribution of labeled species reported in ^{18}O-exchange experiments where substrate concentrations were varied (Hackney et al., 1979; Stroop & Boyer, 1985; Sines & Hackney, 1986), though further comments on this question exceed the reach of this paper.

The study reported here underlines the presence of a random order of binding for ADP and P_i at the active site of the F_oF_1-ATPase, as previously deduced by Kayalar et al. (1977). According to Figure 9, this will be the case for the site with low affinity (site 2). However, these binding properties cannot necessarily be extrapolated for the site with higher affinity (site 1), where a compulsory order of binding, with ADP binding first, could well occur. This, in principle, would agree with the fact that P_i can only bind with high affinity to a site in isolated mitochondrial F_1 which already contains tightly bound ADP (Kozlov & Vulfson, 1985) and could also be compatible with the results obtained when analogues of ADP and/or P_i were used to inhibit photophosphorylation in chloroplasts (Selman & Selman-Reimer, 1981). The much slower release of ADP than of P_i detected during "unisite" catalysis in mitochondrial F_oF_1-ATPase (Grubmeyer et al., 1982; Penefsky, 1985b) also seems to be in line with this hypothesis.

The binding change mechanism discussed for the F_oF_1-ATPase offers an adequate framework to attempt an explanation for the negligible rate of ATP hydrolysis catalyzed by the F_oF_1-ATPase from *P. denitrificans* [Table II; also Ferguson et al. (1976) and Harris et al. (1977)]. The fact that this enzyme is capable of catalyzing much higher rates of ATP $\rightleftharpoons$ P_i exchange than of ATP hydrolysis (Table II) suggests very strongly that the rate-limiting factor of the latter is the slow release of tightly bound ADP from the active site. It is therefore sufficient to assume that, in the case of the F_oF_1-ATPase from *P. denitrificans*, the further binding of ATP to a second site of lower affinity fails to promote the large increase in the rate of product (ADP) release which takes place in the mitochondrial enzyme in the transition from unisite to multisite catalysis (Cross et al., 1982; Penefsky, 1985b). This particular behavior falls in line with the fact that *P. denitrificans* cannot grow by fermentation in the absence of electron acceptors for its respiratory chain (John & Whatley, 1977) and does not require the F_oF_1-ATPase to hydrolyze ATP and generate a protonmotive force, Δp.

The mechanistic interpretation of the experimental values of K_m^{ADP} and $K_m^{P_i}$ is a very important aspect of the findings reported in this paper (see Appendix I). The flux control coefficient of the F_oF_1-ATPase (equal to 1) deduced from titrations with the energy-transfer inhibitor venturicidin (Table I and Figure 3) not only gives full validity to the kinetic analysis used here but also prompts consideration of the actual factors behind any variations in the Michaelis constants observed under different conditions. In this sense, alterations in the rate of release of product (ATP) from the active site of the enzyme are likely to play a crucial role, as this step of the phosphorylating reaction has the largest demand for energy supply [e.g., Boyer et al. (1973) and Penefsky (1985a,b,c)].

As shown in this paper, the properties of the F_oF_1-ATPase from *P. denitrificans* are particularly useful in determining the real affinity for ATP during net ATP synthesis. A further and logical step in this study is to investigate how modulation of energy input and coupling during oxidative phosphorylation affects this affinity. Results attempting to develop this point are presented in the following paper (Pérez & Ferguson, 1990).

Acknowledgments

We thank Dr. David A. Fell (School of Biological and Molecular Sciences, Oxford Polytechnic, Oxford, U.K.) for his contribution in providing the analysis presented in Appendix I. His cooperation is duly appreciated. We also thank Dr. Jean-Pierre Mazat (Université BORDEAUX II, Bordeaux, France) for his interest and personal correspondence. John Elder, Department of Biochemistry, University of Oxford, performed the computer-aided analysis of progress curves included in this paper.

Appendix I: Mechanistic Significance of Experimental Values of K_m^{ADP} ($K_m^{P_i}$)

In analyzing the reaction of ATP synthesis catalyzed by F_oF_1-ATPases, it can be assumed for simplicity that the intrinsic response of the enzyme itself to changes in substrate concentration is hyperbolic and independent of other factors

of the system, such as Δp. As a result, when one of the two substrates, ADP or P_i, is present in saturating amounts, it can be shown that

$$v_F = V_P s/(K_m + s) = V_P/(1 + K_m/s) \quad (A1)$$

where v_F is the catalytic rate of the active complexes of F_oF_1-ATPase, s represents the concentration of the nonsaturating substrate and K_m its Michaelis constant, and V_P is the maximal rate of these operating complexes. Simultaneously, it can be assumed that the "system phosphorylation flux", v, responds to the F_oF_1-ATPase activity in a rectangular hyperbolic manner, whereby the flux control coefficient of this enzyme can vary from values near 1 at low activities toward 0 at high activities. Although there is no theoretical basis for this assumption unless all the processes in the pathway exhibit first-order kinetics (Kacser & Burns, 1979; Waley, 1964), several experimental studies of the variation of metabolic flux with one enzyme activity, at constant levels of the other activities, have shown reasonable agreement with a rectangular hyperbolic function (Dean et al., 1986; Salter et al., 1986; Torres et al., 1986). Therefore

$$v = (V_{obs}v_F)/(K + v_F) = V_{obs}/(1 + K/v_F) \quad (A2)$$

where V_{obs} is the maximum rate which would be observed with an excess of F_oF_1-ATPase activity and K is the parameter which determines the hyperbolic relationship. Equation A2 accounts easily for changes in the flux control coefficient of the F_oF_1-ATPase (see above). K and V_{obs} will be functions of other molecular parameters of the rest of the system and can be considered variables. Therefore, their dependence on those parameters will dictate the overall behavior of the pathway.

By use of eqs A1 and A2, the measurable rate of phosphorylation, v, will be given as

$$v = V_{obs}/[1 + (K/V_P)(1 + K_m/s)] = ({}^{app}V_P s)/({}^{app}K_m + s) \quad (A3)$$

where

$${}^{app}V_P = (V_{obs}V_P)/(V_P + K) \quad (A4)$$

and

$${}^{app}K_m = (K_m K)/(V_P + K) \quad (A5)$$

Equation A3 provides a pseudo-Michaelian dependence of v on s which is directly affected by the value of V_{obs} and K, but more importantly by the relative values of K and V_P. The observation made by Petronilli et al. (1988) of a flux control coefficient equal to 1 for the F_oF_1-ATPase corresponds to the system operating on the region of the hyperbola defined by eq A3, where $K \gg V_P$, as can be concluded by examination of eqs A1 and A2. From eqs A4 and A5 it can be deduced, therefore, that ${}^{app}V_P \rightarrow V_P(V_{obs}/K)$ and that ${}^{app}K_m \rightarrow K_m$. This means that the experimental determinations of ${}^{app}K_m$ will correspond to the real values of the Michaelis constants for the enzyme. On the other hand, ${}^{app}V_P$ will not be a real enzymatic parameter but a global response of the whole pathway.

Equation A5 provides a very simple way of analyzing the effect that a partial inhibition of the F_oF_1-ATPase has on the experimental values of K_m^{ADP} and $K_m^{P_i}$. This can be simulated by substituting V_P for αV_P, where α represents a fractional factor of value within the range $\alpha = 0$–1. Equation A5 shows clearly that, for a given set of parameters (K_m, K), a partial inhibition of the enzyme ($\alpha < 1$) will always increase the value of ${}^{app}K_m$, unless $K \gg V_p$, that is, unless the flux control coefficient of the enzyme is equal to 1, in which case ${}^{app}K_m = K_m$. Therefore, the fact that venturicidin inhibits the F_oF_1-ATPase from *P. denitrificans* without having any effect on K_m^{ADP} or $K_m^{P_i}$ (Table I) directly implies that the enzyme is fully rate limiting and that the experimental values of K_m^{ADP} and $K_m^{P_i}$ are the values of the real Michaelis constants.

The titrations with venturicidin shown in Figure 3 indicate that the affinity of the F_oF_1-ATPase for the inhibitor is affected by membrane energization, presumably due to generation of Δp. For this reason, it is necessary to analyze what effect a positive dependence of the affinity for venturicidin on Δp will have on the experimental determination of K_m^{ADP} and $K_m^{P_i}$ (Table I). This is the case because of the variations of Δp with changes in substrate concentration when the rate of phosphorylation is being measured: as pointed out by Quick and Mills (1987, 1988), a lower substrate concentration is always associated with a higher value of Δp during electron transfer driven ATP synthesis; this is so unless the system is greatly uncoupled and the flux of protons through the F_oF_1-ATPase is small relative to the total flux through the membrane. For this reason, if the affinity for venturicidin increased with Δp, when substrate concentration is being changed for a K_m analysis in the presence of the inhibitor, the extent of inhibition would be greater the lower the substrate concentration. It is very easy to understand that, as a consequence, the observed "apparent" value of the Michaelis constant would be even greater than the one measured if the affinity for the inhibitor had remained constant throughout. Therefore, the lack of increases in K_m^{ADP} and $K_m^{P_i}$ observed with partial inhibition by venturicidin (Table I) cannot be explained by the presumed changes in affinity. This implies that, as concluded before, the flux control coefficient of the enzyme is equal to 1 and the measured K_m^{ADP} and $K_m^{P_i}$ are the real parameters. It is also implied that the affinity for venturicidin does not change for the corresponding range of Δp values.

Equation A2 represents an additional basis for interpretation of the titrations with venturicidin carried out in the presence and absence of rotenone, which are shown in Figure 3B. At saturating substrate concentrations ($v_F = V_P$), the fraction of the observable rate remaining after partial inhibition by venturicidin will be given by

$$v_\alpha/v = \alpha(K + V_P)/(K + \alpha V_P) \quad (A6)$$

where v_α and v represent the rates in the presence and absence of venturicidin, respectively, and α is the fractional parameter defined as before. For the titration carried out in the absence of rotenone, the enzyme is fully rate limiting ($K \gg V_P$), as seen before, so it can be deduced that $v_\alpha/v = \alpha$. For the extent of reduction in the observable rate, due to inhibition by venturicidin (v_α/v), to be the same in both the presence and the absence of rotenone, as shown in Figure 3B, the following equation must be satisfied:

$$v_\alpha/v = \alpha_1 = \alpha_2(K_2 + V_P)/(K_2 + \alpha_2 V_P) \quad (A7)$$

where the subscripts 1 and 2 indicate parameters for the titrations in the absence and in the presence of rotenone, respectively. Equation A7 can be rearranged so that

$$\alpha_2 = (\alpha_1 K_2)/[K_2 + V_P(1 - \alpha_1)] \quad (A8)$$

Two different sets of solutions satisfy eq A8: (i) $K_2 \gg V_P$ and $\alpha_2 = \alpha_1$; that is, the F_oF_1-ATPase is fully rate limiting in the presence of rotenone (as it was in its absence) and the affinity for venturicidin remains unmodified. (ii) K_2 is not much bigger than V_P (the enzyme is not fully rate limiting anymore), in which case $\alpha_2 < \alpha_1$ (greater affinity for venturicidin in the presence of rotenone). However, the second possibility is incompatible with the results shown in Figure 3, as they imply

that the affinity for venturicidin is enhanced by higher levels of energization, and not reduced. Therefore, it can be concluded that in the presence of rotenone the F_oF_1-ATPase is also fully rate limiting and the experimental values of K_m^{ADP} and $K_m^{P_i}$ are real ones.

Appendix II: Kinetic Analysis of F_oF_1-ATPase as a Two-Substrate Enzyme: Order of Binding for ADP and P_i Is a Determinant of the Extent of Product Inhibition

When the F_oF_1-ATPase is taken as a two-substrate enzyme, in the absence of any product inhibition, the corresponding rate equation for the forward reaction can be written as

$$v = V_{max}/[1 + K_m^{P_i}/[P_i] + K_m^{ADP}/[ADP] + (K_i^{P_i}K_m^{ADP})/([P_i][ADP])] \quad (A9)$$

V_{max} represents the maximal rate of phosphorylation; $K_m^{P_i}$ and K_m^{ADP} represent the Michaelis constants for the two substrates; $K_i^{P_i}$ and K_i^{ADP} (which does not appear in eq A9) are the so-called "inhibition constants" for P_i and ADP, respectively, equivalent to the real dissociation constant for binding to the active site (Cornish-Bowden, 1981). The relative values of Michaelis and inhibition constants can be deduced by measuring the rate of phosphorylation for a range of concentrations of one of the substrates, in the presence of several fixed concentrations of the second substrate. Figure 2B shows that, for a range of [ADP], the plots of $t/\ln(a_o/a)$ vs $(a_o - a)/\ln(a_o/a)$, where $a \equiv [P_i]$, produce a family of lines with a common intercept with the x axis. It an be seen that this intercept takes the value (Cornish-Bowden, 1981)

$$-(K_m^{P_i} + K_i^{P_i}K_m^{ADP}/[ADP])/(1 + K_m^{ADP}/[ADP])$$

so a common intercept with the x axis implies that $K_m^{P_i} = K_i^{P_i}$.

Equation A9 is valid whatever the order of binding of ADP and P_i to the enzyme. The situation changes, however, when pure competitive product inhibition is considered. The corresponding rate equations for the forward reaction are as follows:

(*i*) *Random Binding of ADP and P_i.* A rapid equilibrium approach can be used to derive the rate equation (Rudolph, 1979; Cornish-Bowden, 1981):

$$v = dp/dt = V_{max}/[1 + K_m^A/a + K_m^B/b + (K_i^AK_m^B/ab)(1 + p/K_i^P)] \quad (A10)$$

where $A \equiv P_i$, $B \equiv ADP$, $P \equiv ATP$, $a \equiv [P_i]$, $b \equiv [ADP]$, and $p \equiv [ATP]$. Michaelis and inhibition constants will be related by $K_m^AK_i^B = K_i^AK_m^B$.

(*ii*) *Compulsory Order of Binding, with ADP First.* In this case it is more appropriate to apply the King–Altman method, which uses a steady-state approach (Rudolph, 1979; Cornish-Bowden, 1981):

$$v = V_{max}/[1 + K_m^A/a + (K_m^B/b)(1 + p/K_i^P) + (K_i^AK_m^B/ab)(1 + p/K_m^P)] \quad (A11)$$

Michaelis and inhibition constants will now satisfy the relationship $K_i^AK_m^B/K_i^P = K_m^AK_i^B/K_m^P$.

(*iii*) *Compulsory Order of Binding, with P_i First.* Analogous treatment gives

$$v = V_{max}/[1 + (K_m^A/a)(1 + p/K_i^P) + K_m^B/b + (K_i^AK_m^B/ab)(1 + p/K_m^P)] \quad (A12)$$

with the relationship $K_i^AK_m^B/K_m^P = K_m^AK_i^B/K_i^P$.

The Michaelis constant for ATP, K_m^P, appears in both eq A11 and eq A12. However, the fact that the F_oF_1-ATPase from *P. denitrificans* catalyzes almost negligible rates of ATP hydrolysis and rates of ATP $\rightleftharpoons$ P_i exchange much lower than those of ATP synthesis implies that the Michaelis and inhibition constants for ATP must be very similar, if not identical: $K_m^{ATP} \simeq K_i^{ATP}$. Therefore, given that $K_m^{P_i} = K_i^{P_i}$, as mentioned before, we can assume that in all three cases (and not only when random binding occurs) $K_m^{ADP} = K_i^{ADP}$.

A direct comparison of eqs A10–A12 shows that only when ADP and P_i bind randomly to the enzyme does occupancy of the active site by either substrate protect against product inhibition. The application of eqs A10–A12 to the analysis of product inhibition shown in Figure 6 reveals the quantitative differences in the determination of K_i^{ATP} between the three possible orders of binding (see Table III).

(*A*) *ADP as Variable Substrate.* Equation 2 (see Materials and Methods) was used when the initial concentration of P_i was high enough to remain effectively constant during the progress of the phosphorylating reactions (Figure 5A). Taking into account that $a = a_o - p \simeq a_o$, $b = b_o - p$, and $p = p + p_o$ (p_o represents the initial concentration of ATP in the reaction mixtures), eqs A10–A12 can be integrated in the interval $(0, t) \rightarrow (0, p)$ to produce eq 2, where the apparent parameters ${}^{app}V_{max}$ and ${}^{app}K_m^B$ are given as follows:

(*i*) *Random Binding of ADP and P_i.*

$${}^{app}V_{max} = \frac{V_{max}}{1 + (K_m^A/a_o)(1 - K_i^B/K_i^P)} \quad (A13)$$

$${}^{app}K_m^B = K_m^B\frac{1 + (K_i^A/a_o)[1 + (b_o + p_o)/K_i^P]}{1 + (K_m^A/a_o)(1 - K_i^B/K_i^P)} \quad (A14)$$

The graphical representation of ${}^{app}K_m^B$ vs $b_o + p_o$ (Figure 6, panel A1) will give, according to eq A14, an intercept with the x axis such that

$${}^{app}K_i^P = K_i^P(1 + a_o/K_i^A) \quad (A15)$$

(*ii*) *Compulsory Binding, ADP First.*

$${}^{app}V_{max} = V_{max}/[1 - K_m^B/K_i^P + (K_m^A/a_o)(1 - K_i^B/K_m^P)] \quad (A16)$$

$${}^{app}K_m^B = K_m^B\{1 + (b_o + p_o)/K_i^P + (K_i^AK_m^P/a_oK_i^P)[1 + (b_o + p_o)/K_m^P]\}/[1 - K_m^B/K_i^P + (K_m^A/a_o)(1 - K_i^B/K_m^P)] \quad (A17)$$

In this case, the intercept with the x axis is such that

$${}^{app}K_i^P = K_i^P\frac{1 + (K_i^A/a_o)(K_m^P/K_i^P)}{1 + K_i^A/a_o} \quad (A18)$$

Given that $K_m^P \simeq K_i^P$, as discussed before, eq A18 gets reduced to ${}^{app}K_i^P = K_i^P$.

(*iii*) *Compulsory Binding, P_i First.*

$${}^{app}V_{max} = V_{max}/\{1 + (K_m^A/a_o)[1 + (p_o + p/2 - K_i^B)/K_i^P]\} \quad (A19)$$

$${}^{app}K_m^B = K_m^B\{1 + (K_i^A/a_o)[1 + (b_o + p_o)/K_i^P]\}/\{1 + (K_m^A/a_o)[1 + (p_o + p/2 - K_i^B)/K_i^P]\} \quad (A20)$$

It can be noticed that both eq A19 and eq A20 contain a term in p that obviously changes during the progress curves. However, as experiments did not show any deviation from linearity (Figure 5), eq 2 has still been applied to this case, for the sake of comparison with the other two. Equation A19 shows that, if this model of binding really occurs, ${}^{app}V_{max}$ should change with p_o, which is not observed experimentally (Figure 6), unless $K_i^P \gg p_o$, though no product inhibition could then

be expected. Also, eq A20 predicts a nonlinear plot of ${}^{app}K_m^B$ vs $b_o + p_o$.

(B) P_i as Variable Substrate. As shown in Table V, high concentrations of ADP have an inhibitory effect on the binding of P_i. In experiments where low concentrations of P_i and high concentrations of ADP were present (Figure 6, panel B1), this effect was important and had to be accounted for. In the absence of product inhibition, eq A9 can be expanded to include a second binding of ADP, in the form

$$v = V_{max}/[1 + K_m^B/b + (K_m^A/a)(1 + K_i^B/b + b/K_i^{B'})] \quad (A21)$$

where $K_i^{B'}$ represents the new constant of competitive inhibition by ADP on the binding of P_i. In experiments such as the one shown in Table V, where different but saturating (for $K_m^B = K_i^B$) concentrations of ADP were used, ${}^{app}K_m^A = K_m^A(1 + b/K_i^{B'})$. The values of ${}^{app}K_m^A$ are provided by the intercept with the x axis of the plots of $t/\ln(a_o/a)$ vs $(a_o - a)/\ln(a_o/a)$. From the experiment shown in Table V, a value of $K_i^{B'} = 2.6$ mM can be deduced, similar to the inhibition constant previously characterized for the F_oF_1-ATPase from chloroplasts (Selman & Selman-Reimer, 1981).

As mentioned before (see Results), the progress curves for product inhibition in the presence of low $[P_i]_o$ and high $[ADP]_o$ fitted eq 3 surprisingly well (solid lines in Figure 6, panel B1). Such a "pseudo-monosubstrate" pattern was better analyzed by applying eq 2 to the reaction with no ATP added and comparing the result to a control reaction which included hexokinase and glucose (Table V): the acceleration of the reaction due to the continuous decrease in [ADP] (and, therefore, the progressive increase in the apparent affinity for P_i) resulted in a set of "pseudoapparent" parameters V_{max} and $K_m^{P_i}$ which were smaller than the ones derived from the control reaction. The pseudoapparent values of V_{max} and $K_m^{P_i}$ computed for each of the progress curves of Figure 6, panel B1 (a fixed V_{max} was used, according to pure competitive product inhibition), were used to obtain the initial rates by extrapolation, applying the simplest Michaelian equation

$$v_o = ({}^{app}V_{max}[P_i]_o)/({}^{app}K_m^{P_i} + [P_i]_o)$$

where v_o indicates the initial rate. These initial rates, in turn, were used to derive the corresponding range of values of ${}^{app}K_m^{P_i}$ (changes in ${}^{app}K_m^{P_i}$ are due only to increasing [ATP]) with

$${}^{app}K_m^{P_i} = [P_i]_o(V_{max}/v_o - 1)$$

where V_{max} corresponds to the maximal rate associated with the control reaction in the presence of hexokinase and glucose (Table V).

The inhibition of P_i binding by ADP ($K_i^{B'}$) can be included in eqs A10–A12, where pure competitive product inhibition is also considered. The new equations can then be used to analyze the plot of ${}^{app}K_m^{P_i}$ vs [ATP] shown in Figure 6, panel B2; the intercept with the x axis ($-{}^{app}K_i^P$) will be a function of the real K_i^P and the degree of occupancy of the two binding sites for ADP. This will depend on the type of binding for ADP and P_i as follows:

(i) Random Binding of ADP and P_i.

$${}^{app}K_i^P = K_i^P[1 + (b_o/K_i^B)(1 + b_o/K_i^{B'})] \quad (A22)$$

(ii) Compulsory Binding, ADP First.

$${}^{app}K_i^P = K_i^P[1 + (b_o/K_i^B)(1 + b_o/K_i^{B'})] \quad (A23)$$

(iii) Compulsory Binding, P_i First.

$${}^{app}K_i^P = K_i^P[1 + (b_o/K_i^{B'})/(1 + K_i^B/b_o)] \quad (A24)$$

It should be noted that eqs A22 and A23 are identical.

Registry No. ATP, 56-65-5; ADP, 58-64-0; P_i, 14265-44-2; ATPase, 9000-83-3; ATP synthase, 37205-63-3.

References

Atkins, G. L., & Nimmo, I. A. (1973) *Biochem. J. 135*, 779–784.

Ballard, A. (1988) Ph.D. Thesis, University of Birmingham.

Boyer, P. D. (1989) *FASEB J. 3*, 2164–2178.

Boyer, P. D., Cross, R. L., & Momsen, W. (1973) *Proc. Natl. Acad. Sci. U.S.A. 70*, 2837–2839.

Brand, M. D., & Lehninger, A. L. (1977) *Proc. Natl. Acad. Sci. U.S.A. 74*, 1955–1959.

Burnell, J. N., John, P., & Whatley, F. R. (1975) *Biochem. J. 150*, 527–536.

Choate, G. L., Hutton, R. L., & Boyer, P. D. (1979) *J. Biol. Chem. 254*, 286–290.

Cornish-Bowden, A. (1981) *Fundamentals of Enzyme Kinetics*, Butterworths, London.

Cross, R. L. (1981) *Annu. Rev. Biochem. 50*, 681–714.

Cross, R. L., Grubmeyer, C., & Penefsky, H. S. (1982) *J. Biol. Chem. 257*, 12101–12105.

Dean, A. M., Dykhuizen, D. E., & Hartl, D. L. (1986) *Genet. Res. 48*, 1–8.

Eilermann, L. J. M., & Slater, E. C. (1970) *Biochim. Biophys. Acta 216*, 226–228.

Ferguson, S. J. (1975) D.Phil. Thesis, University of Oxford.

Ferguson, S. J., & John, P. (1977) *Biochem. Soc. Trans. 5*, 1525–1527.

Ferguson, S. J., John, P., Lloyd, W. J., Radda, G. K., & Whatley, F. R. (1976) *FEBS Lett. 62*, 272–275.

Fernley, H. N. (1974) *Eur. J. Biochem. 43*, 377–378.

Franek, U., & Strotmann, H. (1981) *FEBS Lett. 126*, 5–8.

Gresser, M. J., Myers, J. A., & Boyer, P. D. (1982) *J. Biol. Chem. 257*, 12030–12038.

Grubmeyer, C., Cross, R. L., & Penefsky, H. S. (1982) *J. Biol. Chem. 257*, 12092–12100.

Hackney, D. D., & Boyer, P. D. (1978) *J. Biol. Chem. 253*, 3164–3170.

Hackney, D. D., Rosen, G., & Boyer, P. D. (1979) *Proc. Natl. Acad. Sci. U.S.A. 76*, 3646–3650.

Harris, D. A., John, P., & Radda, G. K. (1977) *Biochim. Biophys. Acta 459*, 546–559.

Heinrich, R., & Rapoport, T. A. (1974) *Eur. J. Biochem. 42*, 89–95.

Hekman, C., Matsuno-Yagi, A., & Hatefi, Y. (1988) *Biochemistry 27*, 7559–7560.

Herweijer, M. A., Berden, J. A., Kemp, A., & Slater, E. C. (1985) *Biochim. Biophys. Acta 809*, 81–89.

John, P. (1977) *J. Gen. Microbiol. 98*, 231–238.

John, P., & Whatley, F. R. (1977) *Biochim. Biophys. Acta 463*, 129–153.

Kacser, H., & Burns, J. A. (1973) *Symp. Soc. Exp. Biol. 27*, 65–104.

Kacser, H., & Burns, J. A. (1979) *Biochem. Soc. Trans. 7*, 1149–1160.

Kayalar, C., Rosing, J., & Boyer, P. D. (1976) *Biochem. Biophys. Res. Commun. 72*, 1153–1159.

Kayalar, C., Rosing, J., & Boyer, P. D. (1977) *J. Biol. Chem. 252*, 2486–2491.

Kozlov, I. A., & Vulfson, E. N. (1985) *FEBS Lett. 182*, 425–428.

Lemasters, J. J., & Fleishman, K. E. (1987) *Biochem. Biophys. Res. Commun. 142*, 176–182.

Linnett, P. E., & Beechey, R. B. (1979) *Methods Enzymol. 55*, 472–518.

Lowry, O. H., Rosebrough, N. J., Farr, A. L., & Randall, R. J. (1951) *J. Biol. Chem. 193*, 265-275.
Magnusson, R. P., & McCarty, R. E. (1976) *J. Biol. Chem. 251*, 7417-7422.
Mathews, C. K. (1972) *J. Biol. Chem. 247*, 7430-7438.
Matsuno-Yagi, A., & Hatefi, Y. (1985) *J. Biol. Chem. 260*, 14424-14427.
Matsuno-Yagi, A., & Hatefi, Y. (1986) *J. Biol. Chem. 261*, 14031-14038.
McCarthy, J. E. G., & Ferguson, S. J. (1983) *Eur. J. Biochem. 132*, 417-424.
Nicholls, D. G. (1982) *Bioenergetics*, Academic Press, London.
Orsi, B. A., & Tipton, K. F. (1979) *Methods Enzymol. 63*, 159-183.
O'Sullivan, W. J., & Smithers, G. W. (1979) *Methods Enzymol. 63*, 294-336.
Parsonage, D. (1984) Ph.D. Thesis, University of Birmingham.
Penefsky, H. S. (1985a) *Proc. Natl. Acad. Sci. U.S.A. 82*, 1589-1593.
Penefsky, H. S. (1985b) *J. Biol. Chem. 260*, 13728-13734.
Penefsky, H. S. (1985c) *J. Biol. Chem. 260*, 13735-13741.
Pérez, J. A., & Ferguson, S. J. (1990) *Biochemistry* (following paper in this issue).
Pérez, J. A., Greenfield, A. J., Sutton, R., & Ferguson, S. J. (1986) *FEBS Lett. 198*, 113-118.
Petronilli, V., Pietrobon, D., Zoratti, M., & Azzone, G. F. (1986) *Eur. J. Biochem. 155*, 423-431.
Petronilli, V., Azzone, G. F., & Pietrobon, D. (1988) *Biochim. Biophys. Acta 932*, 306-324.
Quick, W. P., & Mills, J. D. (1987) *Biochim. Biophys. Acta 893*, 197-207.
Quick, W. P., & Mills, J. D. (1988) *Biochim. Biophys. Acta 932*, 232-239.
Rosing, J., & Slater, E. C. (1972) *Biochim. Biophys. Acta 267*, 275-290.
Rosing, J., Kayalar, C., & Boyer, P. D. (1977) *J. Biol. Chem. 252*, 2478-2485.
Rudolph, F. B. (1979) *Methods Enzymol. 63*, 411-436.
Salter, M., Knowles, R. G., & Pogson, C. I. (1986) *Biochem. J. 234*, 635-647.
Schuster, S., Reinhart, G. D., & Lardy, H. A. (1977) *J. Biol. Chem. 252*, 427-432.
Selman, B. R., & Selman-Reimer, S. (1981) *J. Biol. Chem. 256*, 1722-1726.
Senior, A. E. (1988) *Physiol. Rev. 68*, 177-231.
Sines, J. J., & Hackney, D. D. (1986) *Biochemistry 25*, 6144-6149.
Sorgato, M. C., Ferguson, S. J., Kell, D. B., & John, P. (1981) *Biochem. J. 174*, 237-256.
Stoner, C. D. (1984) *J. Bioenerg. Biomembr. 16*, 115-141.
Storer, A. C., & Cornish-Bowden, A. (1976) *Biochem. J. 159*, 1-5.
Stroop, S. D., & Boyer, P. D. (1985) *Biochemistry 24*, 2304-2310.
Sugino, Y., & Miyoshi, Y. (1964) *J. Biol. Chem. 239*, 2360-2364.
Taussky, H. H., & Shorr, E. (1953) *J. Biol. Chem. 202*, 675-685.
Torres, N. V., Mateo, F., Meléndez-Hevia, E., & Kacser, H. (1986) *Biochem. J. 234*, 169-174.
Waley, S. G. (1964) *Biochem. J. 91*, 514-517.

Kinetics of Oxidative Phosphorylation in *Paracoccus denitrificans*. 2. Evidence for a Kinetic and Thermodynamic Modulation of F_oF_1-ATPase by the Activity of the Respiratory Chain†

Juan A. Pérez* and Stuart J. Ferguson
Department of Biochemistry, University of Oxford, South Parks Road, Oxford OX1 3QU, U.K.
Received August 9, 1989; Revised Manuscript Received July 25, 1990

ABSTRACT: (1) The affinity of the F_oF_1-ATPase from *Paracoccus denitrificans* for ATP during NADH-driven oxidative phosphorylation has been analyzed under different conditions by examining the type and extent of product inhibition. (2) A limited collapse of the protonmotive force (Δp) due to partial uncoupling does not increase the affinity for ATP at the active site(s) of the enzyme; instead, a partial noncompetitive inhibition becomes apparent, compatible with the binding of ATP to a noncatalytic site (or sites) with high affinity. (3) In contrast, partial inhibition of the electron-transport chain increases the extent of pure competitive product inhibition and, therefore, the affinity for ATP at the active site(s). (4) The results are interpreted as indicative of a modulation of the rate of ATP release from the active site(s) of the F_oF_1-ATPase which is controlled by the activity of the electron-transport chain and not by Δp.

In the mechanism of ATP synthesis catalyzed by F_oF_1-ATPases,[1] the release of ATP from the active site(s) is considered to be the step with the largest demand for energy [e.g., Boyer et al. (1973) and Hackney et al. (1979)]. In agreement with this idea, the onset of respiration in beef heart submitochondrial particles was observed to reduce dramatically the affinity for ATP at the active site of the F_oF_1-ATPase (Penefsky, 1985). According to the simplest delocalized version

† J.A.P. was supported by a research fellowship from the Departamento de Educación, Universidades e Investigación, Gobierno Vasco/Eusko Jaurlaritza, Spain.

[1] Abbreviations: Δp, protonmotive force or transmembrane electrochemical proton gradient expressed in millivolts; F_oF_1-ATPase, H^+-translocating ATPase type F_oF_1 (ATP-synthase; EC 3.6.1.3); F_1, soluble catalytic sector of F_oF_1-ATPase; P_i, inorganic phosphate; G6P, glucose 6-phosphate; HK, hexokinase; FCCP, carbonyl cyanide *p*-(trifluoromethoxy)phenylhydrazone.

0006-2960/90/0429-10518$02.50/0